Hierarchy of RNA Functional Dynamics

Anthony M. Mustoe,[1] Charles L. Brooks,[1,2] and Hashim M. Al-Hashimi[3]

Departments of [1]Biophysics and [2]Chemistry, University of Michigan, Ann Arbor, Michigan 48109-105; email: brookscl@umich.edu

[3]Department of Biochemistry and Chemistry, Duke University Medical Center, Durham, North Carolina 27710; email: hashim.al.hashimi@duke.edu

Annu. Rev. Biochem. 2014. 83:441–66

First published online as a Review in Advance on March 5, 2014

The *Annual Review of Biochemistry* is online at biochem.annualreviews.org

This article's doi: 10.1146/annurev-biochem-060713-035524

Keywords

RNA flexibility, riboswitches, regulatory RNA, molecular adaptation, RNA catalysis

Abstract

RNA dynamics play a fundamental role in many cellular functions. However, there is no general framework to describe these complex processes, which typically consist of many structural maneuvers that occur over timescales ranging from picoseconds to seconds. Here, we classify RNA dynamics into distinct modes representing transitions between basins on a hierarchical free-energy landscape. These transitions include large-scale secondary-structural transitions at >0.1-s timescales, base-pair/tertiary dynamics at microsecond-to-millisecond timescales, stacking dynamics at timescales ranging from nanoseconds to microseconds, and other "jittering" motions at timescales ranging from picoseconds to nanoseconds. We review various modes within these three different tiers, the different mechanisms by which they are used to regulate function, and how they can be coupled together to achieve greater functional complexity.

Contents

INTRODUCTION 442
DECOMPOSING RNA DYNAMICS INTO HIERARCHICAL MOTIONS 442
TIER 0: SECONDARY-STRUCTURE DYNAMICS 444
Overview 444
Biological Significance 444
TIER 1: BASE-PAIR AND TERTIARY DYNAMICS 446
Base-Pair Melting 447
Base-Pair Reshuffling 448
Base-Pair Isomerization 449
Tertiary-Structure Dynamics 450
TIER 2: JITTERING DYNAMICS ... 452
Interhelical Dynamics 452
Loop Dynamics 454
INTERDEPENDENCE OF SUBSTATES ACROSS TIERS 455
Secondary-Structure and Tertiary-Structure Dynamics 455
Tertiary Structure and Loop Dynamics 457
Tertiary Structure and Interhelical Dynamics 457
Base Reshuffling and Interhelical Dynamics 457
CONCLUSIONS 458

INTRODUCTION

Composed of only four chemically similar nucleotides, RNA was long thought to lack the chemical and structural complexity needed to drive the biochemical processes that power living cells; rather, it was considered to be limited to a role as a rudimentary messenger. However, discoveries in molecular biology made during the past three decades have shown that nothing could be further from the truth. RNA is capable of catalytic activity and can fold into complex three-dimensional (3D) structures rivaling those of proteins (1–5). We now believe that 75% of the human genome is transcribed into RNA, yet less than 2% codes for proteins (6, 7). The function of most of these transcribed RNAs has yet to be uncovered. Even classic RNAs such as ribosomal (rRNAs), transfer (tRNAs), and messenger RNAs (mRNAs) play surprisingly complex roles in protein synthesis (5, 8).

The functional complexity of RNA and its involvement in a wide range of sophisticated biological processes can be attributed not only to its ability to fold into complex 3D structures but, perhaps even more importantly, to its ability to undergo precise conformational changes in response to a wide range of specific cellular cues consisting of proteins, ligands, metals, changes in temperature, and pH (9, 10). These dynamics can be highly complex, often involving many structural maneuvers that take place over timescales ranging from picoseconds to hundreds of seconds. What is lacking is a framework for simplifying this dazzling complexity so that one can begin to comprehend the signal within the noise.

In this review, we introduce a framework for deconstructing RNA dynamics into a set of distinct motional modes that have characteristic timescales representing transitions between basins within a hierarchical free-energy landscape. This framework simplifies the description of complex RNA dynamics in terms of a set of recurring motional modes, providing a common language that enables one to identify similar themes across different RNA functional contexts, and is very similar to that first introduced by Frauenfelder et al. (11) to describe protein dynamics. We review three broad classes of RNA dynamics, their biological significance, and how interdependencies among these classes can be harnessed to achieve even greater functional complexity.

DECOMPOSING RNA DYNAMICS INTO HIERARCHICAL MOTIONS

In solution, a given RNA does not fold into a single structure but rather forms a statistical distribution, or ensemble, of many interconverting

conformations. As with proteins, this statistical ensemble can be described in terms of a continuous free-energy landscape, which specifies the free energy of every atomic configuration (11). The population of each configuration depends on its free energy, whereas the rates of interconversion between individual configurations depend on the height of the barriers separating them. Although the free-energy landscape can in principle be arbitrarily complex, in many biomolecules it is hierarchically organized into local energetic minima containing conformational substates (CSs) that are separated by large barriers, each of which is, in turn, subdivided into a greater number of local energetic minima that are separated by lower barriers, and so forth (**Figure 1**). These hierarchically organized energetic layers form different tiers (Tier 0, Tier 1, and so on), and RNA dynamics can be hierarchically organized in terms of transitions between CSs within different tiers.

The above hierarchical description of free-energy landscapes and dynamics was developed originally to explain the dynamics of the protein myoglobin. However, it is also well suited to describing RNA dynamics in general for two reasons. First, the RNA free-energy landscape is strongly hierarchical and is naturally organized into secondary and tertiary structure levels (12, 13). Unlike proteins, interactions that stabilize secondary structure are much stronger than those that stabilize other aspects of 3D structure, and dynamics at the secondary-structure level (Tier 0) occur largely independently of those on lower levels (Tiers 1, 2, etc.). Second, the RNA free-energy landscape is rugged; significant barriers separate alternative conformations at both the secondary- and tertiary-structural levels. Thus, RNA may be described in terms of individual CSs within each tier. In our discussion, Tier 0 refers to RNA conformations with a distinct secondary structure, Tier 1 refers to conformations that have minor differences in base-pairing, and Tier 2 refers to conformations that have similar secondary structures and base-pairing but differ in other aspects of structure (**Figure 1**).

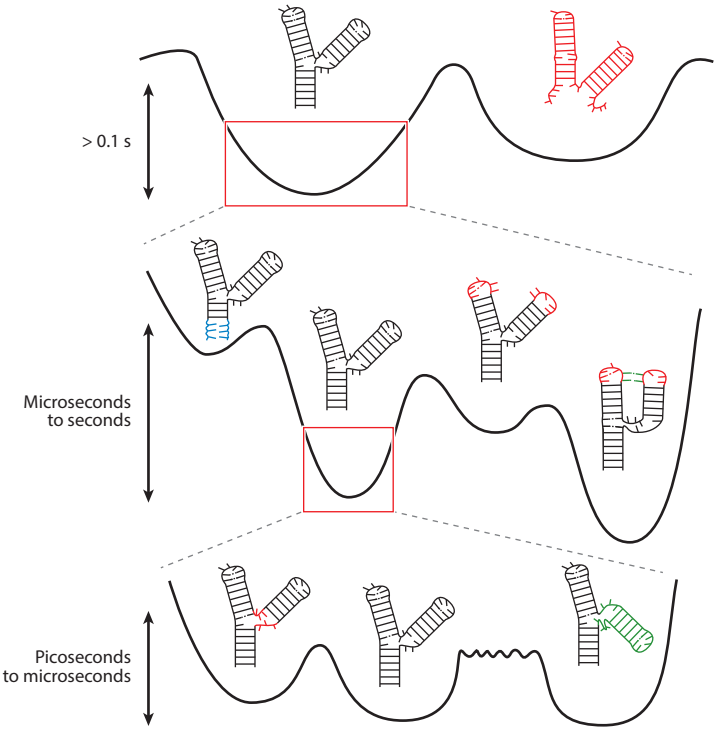

Figure 1

The different tiers of RNA dynamics. At the lowest level of the hierarchy are secondary-structure dynamics, which define broad free-energy basins with high separating barriers. Within each secondary structure are smaller, alternative local base-pairing arrangements that define Tier 1 dynamics. These include base-pair melting (*left*, *blue*), reshuffling (*far right*, *red*), and tertiary pairing (*green*). Each local pairing basin, in turn, defines a limited set of three-dimensional conformations with transitions between these basins constituting Tier 2 dynamics. These dynamics include loop dynamics (*left*, *red*) and interhelical dynamics (*right*, *green*). Although interhelical and loop dynamics have similar barrier heights, due to the larger number of involved coordinates, interhelical dynamics typically occur more slowly (*long rough separating barrier*).

Other than the property of being hierarchal, three other aspects of the RNA free-energy landscape are worth mentioning. First, there is mounting evidence that cellular cues change the energetic balance of preexisting CSs to trigger specific biological outcomes (10). In other words, the favorable CSs that exist in quiescent RNAs represent the same conformations that nature uses to regulate biological outcomes. Second, as we elaborate below, nature takes advantage of the different exchange rates available at different tiers to ensure that conformational

changes occur either (*a*) only once a specific cellular cue is presented or (*b*) sufficiently rapidly so as to not slow down biochemical processes. Finally, although limited in number, the CSs that populate the free-energy landscape can have wildly different conformations, enabling cellular cues to effect large yet highly specific changes in structure. In the following sections, we describe the different tiers of RNA dynamics and discuss their biological significance.

TIER 0: SECONDARY-STRUCTURE DYNAMICS

Overview

Due to the inherent degeneracies of the energetics of base-pairing and stacking, RNA molecules rarely fold into a single secondary structure. Rather, additional competing secondary-structural forms can become appreciably populated under the right physiological conditions (14–16). In sequences that have evolved to favor a single functional conformation, these alternative secondary structures present a challenge to RNA folding (17, 18). However, in other cases, this promiscuous pairing ability is deliberately harnessed to create functional transitions between alternative secondary structures (**Figure 2**).

Because of the overwhelming stability of RNA duplexes, transitions to conformations possessing only slightly fewer pairs are strongly disfavored. Thus, in theory, secondary-structure dynamics can be highly specific, directed to one of a few favorable conformations. However, because a transitioning duplex must typically break half of its base pairs, this stability comes at the cost of slow dynamics timescales (19, 20). For example, transitions of a bistable RNA between two alternative 5-bp helices occur at rates of $\sim$0.1 s^{-1} at 298 K (19). For larger helices, the timescale of interconversion can approach the expected lifetime of the RNA and can be slowed down even further by formation of long-lived intermediates (18, 21–23).

Biological Significance

Nature often exploits dynamics between different secondary structures to sequester or expose functional structural elements in response to cellular cues. This process gives rise to molecular switches, termed riboswitches, that can be integrated into various biological circuits (24). These structural elements may be either (*a*) a contiguous stretch of nucleotides that are exposed as single strands or sequestered into hairpins via base-pairing or (*b*) an entire hairpin that is either present or absent from the secondary structure. For example, single-stranded mRNA ribosome binding sites (25), degradative endonuclease cleavage sites (26) and splicing sites (27), and transcription terminator hairpins (28), among others, are exposed or sequestered by secondary-structure changes as part of regulatory processes (**Figure 2**).

Secondary-structure dynamics present both a challenge (fast response times are often needed to efficiently respond to biological stimuli) and an opportunity (the transitions are

Figure 2

(*a*) Three-state secondary-structure equilibrium of the *add* adenine riboswitch. In the adenine-bound conformation, both the start codon (*green*) and the ribosome binding site (*red*) are exposed, upregulating translation. The temperature dependence of the apo-state secondary-structure equilibrium offsets the increased ligand affinity of the binding-competent conformation at low temperature (31). Rate and equilibrium constants correspond to those measured at 25°C. (*b*) Example of a transcriptional acting adenine riboswitch. Ligand binding stabilizes a transient secondary structure, sequestering residues that would otherwise pair with downstream transcribed sequences to form the thermodynamically favored terminator stem. (*c*) The HIV-1 5′ leader couples exposure of the start codon of the downstream-encoded Gag protein to sequestration of the dimerization initiation site (*red*), promoting translation while inhibiting dimerization (*left*). In a process promoted by the nucleocapsid chaperone protein (NC) (*purple*), the leader undergoes a secondary-structure switch that exposes the dimerization initiation site and sequesters the start codon, attenuating translation and promoting dimerization, which initiates genome packaging (*right*) (41).

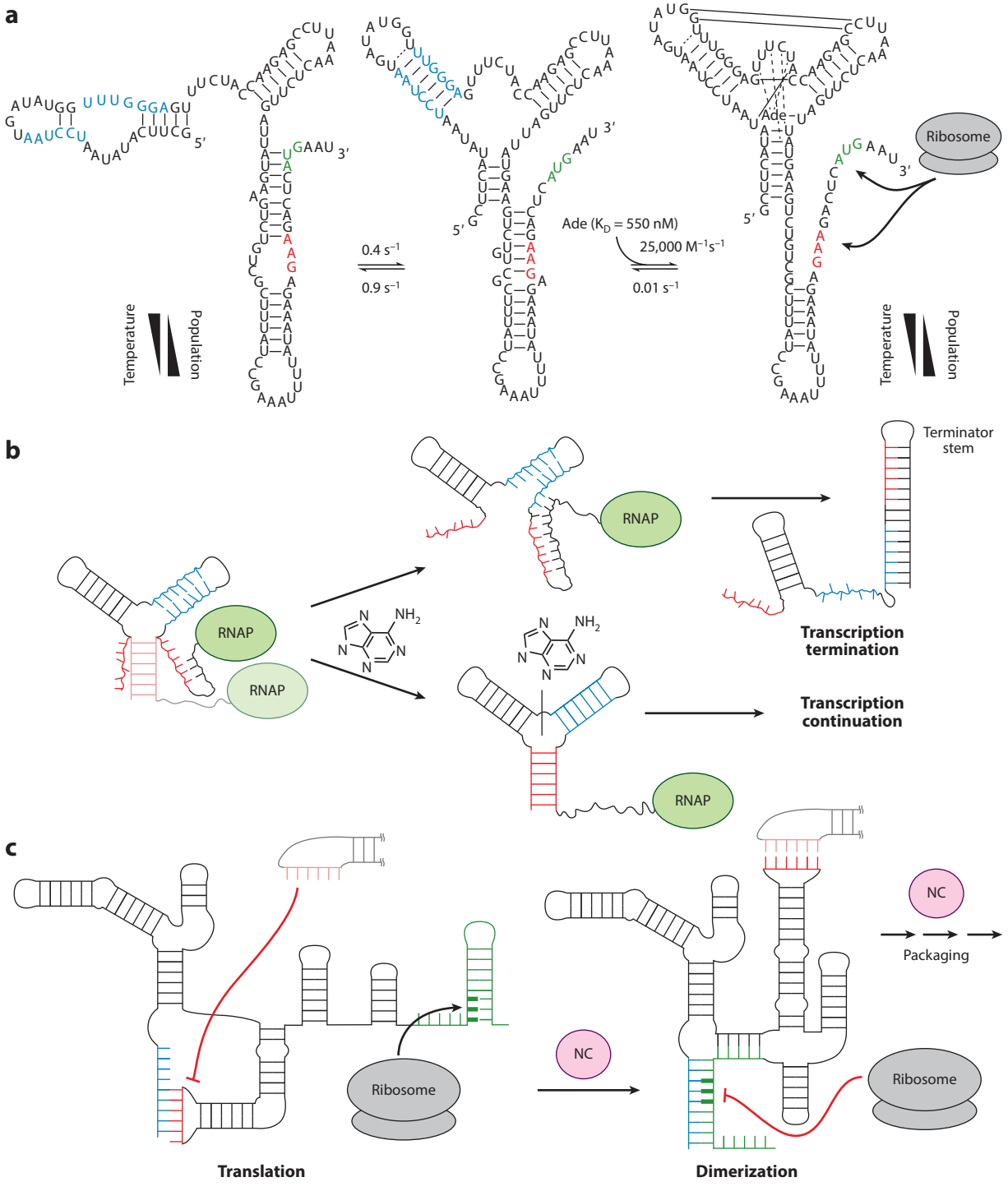

unlikely to occur spontaneously in an undirected manner). Nature has evolved several strategies to overcome this challenge that allow it to exploit the opportunity to construct robust regulatory switches.

Some secondary-structure transitions can be used "as is" without needing to intervene with their rates of interconversion. In such cases, a preexisting secondary-structure equilibrium is precisely tuned by primary sequence to rapidly and reversibly respond to changes in small-molecule concentration (24, 29) or to temperature in so-called thermosensors (30). Many riboswitches that regulate gene expression at the translational level are controlled by such thermodynamic mechanisms. An interesting example is provided by the *add* adenine riboswitch, in which dynamics between three alternative secondary structures collaborate to create an adenine-responsive switch that is active across a broad range of temperatures (31). A temperature-sensitive preequilibrium that exchanges with rates of $\sim$0.5 s^{-1} between two translational off states sequesters the ligand binding pocket to inhibit switching, compensating for the temperature sensitivity of the ligand-modulated equilibrium between translational on and off states (**Figure 2*a***).

In other cases, the barriers between two secondary structures are high enough that exchange cannot occur within reasonable timescales without some form of intervention. For example, rapid secondary-structure transitions are required in riboswitches that regulate gene expression at the transcriptional level, in which the structural change must occur during a short time window dictated by the transcription rate. An ingenious form of intervention involves altering the cotranscriptional folding pathway of an RNA, thereby acting before a stable secondary-structure element has had a chance to fully form. In these cases, a wide range of effectors, such as temperature (32), small molecules (24, 29), metals (33), pH (34), proteins (35), or *trans*-acting RNAs (36), stabilize a metastable secondary structure during cotranscriptional folding that sequesters sequence elements that would otherwise pair with downstream nucleotides emerging from the polymerase (**Figure 2*b***). Not only do such systems allow rapid exchange between conformations that would otherwise be separated by insurmountable energetic barriers, but they also ensure that the conformational switch rarely occurs in the absence of effectors.

Nature has also evolved various protein chaperones and helicases that can both accelerate transitions between more stable secondary structures and time the transitions so that they take place at specific time points. These proteins act by either destabilizing duplexes or stabilizing unpaired states to lower the effective transition barrier (see the section titled Base-Pair Melting, below) (22). For example, such proteins allow the efficient annealing of regulatory small RNAs to potentially structured regions of their mRNA targets (37). During assembly of the eukaryotic spliceosome, helicases are used to catalyze successive global secondary-structure transitions that serve as a multistep proofreading mechanism to ensure that only optimal substrates are spliced (38). These proteins can also serve as regulatory triggers; an increase in protein concentration can promote transitions of RNAs to alternative functional conformations, by either destabilizing a preexisting state or stabilizing a new conformation. This mechanism is prominently used by retroviruses to regulate genome translation, dimerization, and packaging (**Figure 2*c***) (39–41).

TIER 1: BASE-PAIR AND TERTIARY DYNAMICS

Once formed, a given secondary structure may experience smaller, more localized changes in base-pairing, or may form long-range tertiary base-pairing or other interactions between remotely positioned residues. These dynamics do not cause large-scale changes in secondary structure and can therefore be considered basins within a given secondary-structure CS. We distinguish four different types of dynamics: (*a*) base-pair melting, (*b*) base-pair reshuffling, (*c*) base-pair isomerization, and (*d*) long-range tertiary interactions (**Figure 3**).

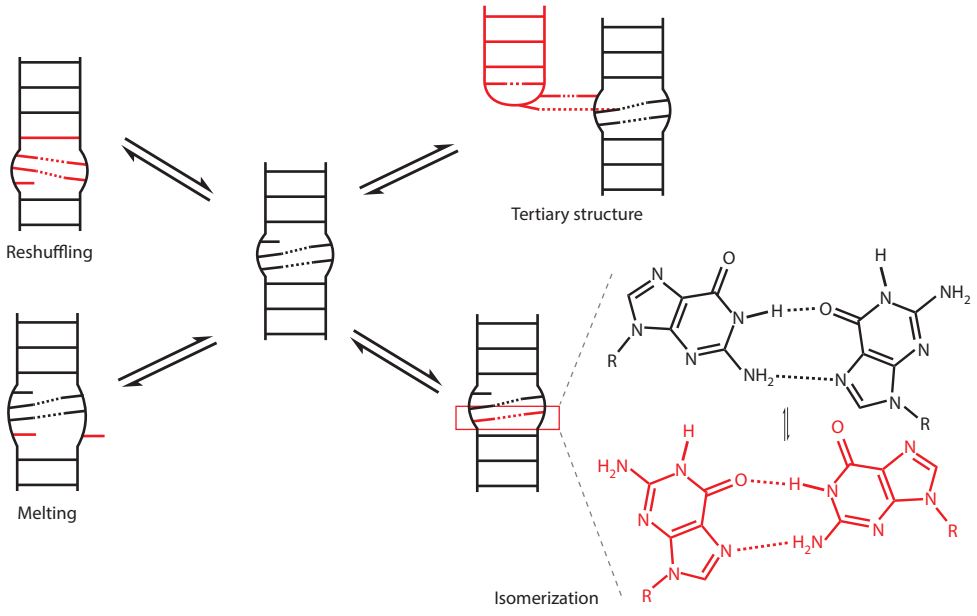

Figure 3

Modes of Tier 1 dynamics.

Base-Pair Melting

Overview. All base pairs, including Watson–Crick (WC) pairs, transiently break apart (melt) and adopt an open conformation that briefly exposes their residues to solvent or nearby binding partners. For WC base pairs, melting occurs on 0.1–50-ms timescales, depending on the identity of the pair and on the strength of the stacking interactions with neighboring base pairs (42, 43). Unlike other forms of base-pair dynamics (reviewed below), the open state is strongly energetically disfavored compared with the paired state (roughly 7–9 kcal/mol for WC pairs in duplex RNA). As a result, at room temperature, the open state of WC base pairs has a minute population of 10^{-5} to 10^{-6} and a lifetime of only 1 to 100 ns (42, 43). However, the population and lifetime of the open state can increase considerably in (*a*) helix-terminating pairs that have only one set of nearest-neighbor stacking interactions, such as base pairs near bulges, apical loops, or internal loops, and (*b*) noncanonical base pairs (43, 44). To a lesser extent, instability in a single pair can also increase the melting dynamics of non-nearest-neighbor pairs, although the mechanisms underlying this phenomenon are not fully understood (44).

Biological significance. Sites of increased transient melting are common trigger points for effecting larger-scale secondary-structure transitions. RNA chaperones and helicases operate by lowering the barriers to melting dynamics and then binding with high affinity to the exposed residues (**Figure 4**) (45, 46). This binding, in turn, enhances the melting dynamics and, therefore, the refolding ability of pairs that neighbor the chaperone–RNA interface.

Melting of weak base pairs can also expose residues that participate in RNA–RNA tertiary interactions and RNA–protein binding motifs (47–50). In an interesting example, in the ribosomal peptidyl transferase center, tertiary interactions with the A-site tRNA induce melting of a G–U pair in the 23S rRNA that otherwise protects the aminoacyl linkage of the P-site tRNA from spontaneous hydrolysis

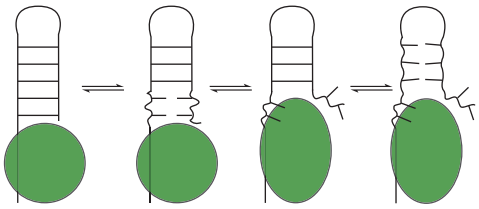

Figure 4

Example of an RNA chaperone (45, 46). The bound chaperone destabilizes the neighboring RNA helix, promoting melting dynamics, and then binds the exposed nucleotides. The other strand is released and can interact with other RNAs, and the remainder of the helix is also destabilized.

(51). Melting dynamics also provide the basis of several regulatory strategies. For example, the interplay between the helicase activity of the ribosome (52) and the melting dynamics of mRNA secondary structure has been proposed to serve as a second genetic code that regulates the rate of ribosomal translocation and, therefore, cotranslational protein folding (53). Similarly, this interplay has been implicated as playing an important role in the mechanism underlying ribosomal frameshifting (54).

Base-Pair Reshuffling

Overview. Base-pair reshuffling dynamics typically involve local rearrangements in base-pairing partners in and around noncanonical structures, such as apical and internal loops (55). The transitions typically require the disruption of one or two noncanonical or unstable base pairs; therefore, they typically occur at microsecond to millisecond timescales, which is similar to or slightly faster than the rate of base-pair opening (55). In general, "reshuffled" states are destabilized relative to the most favorable state by <3 kcal/mol and thus have populations of $\geq 0.5\%$ and lifetimes on the order of >50 μs (55). Compared with global secondary-structure transitions, these more localized changes in base-pairing occur at rates that are nearly three orders of magnitude faster and do not require assistance from cellular factors or cotranscriptional folding.

An example of such dynamics in an apical loop is provided by the HIV-1 *trans*-activation response element (TAR), in which relaxation dispersion NMR spectroscopy has identified two alternatively paired CSs (**Figure 5*a***) (55). In the energetically favored CS, the hexanucleotide apical loop adopts a conformation in which G34 forms a cross-loop WC pair with C30, leaving other nucleotides unpaired. By contrast, the energetically less favorable CS, which has a population of 13%, adopts a tetraloop conformation closed by *trans*-wobble U31–G34 and noncanonical $A35^+$–C30 wobble base pairs (**Figure 5*a***). Prior observations of higher-energy CS states involving $C–A^+$ base pairs in RNA (56–58) and $G–C^+$ Hoogsteen base pairs in DNA (59, 60) suggest that formation of charged base pairs may be a general characteristic of Tier 1 dynamics. The ribosomal A-site represents an example of base-pair reshuffling in an internal loop (**Figure 5*b***) (55). Here, adenine and uridine residues alternate between being exposed as a loop or a bulge or being sequestered through formation of noncanonical base pairs.

Biological significance. As in global secondary-structure transitions, reshuffled CSs can differ in terms of whether certain residues are exposed and available for interaction with cellular cues or sequestered through base-pairing interactions. As a result, they can be employed as expose/sequester switches that are much faster than secondary-structure transitions. Although the function of reshuffling dynamics is still under investigation, several possible biological roles have been proposed.

For example, the higher-energy CS in the TAR apical loop (discussed above) appears to form an autoinhibited state because it sequesters residues that are recognized by transcription factors such as Tat (55). Indeed, mutations that stabilize this CS lead to weaker protein binding affinities and inhibit transcriptional activation (**Figure 5*a***). Because formation of the A^+–C pair in this CS requires protonation, dynamics between the two different CSs depend on pH and thus may serve as a

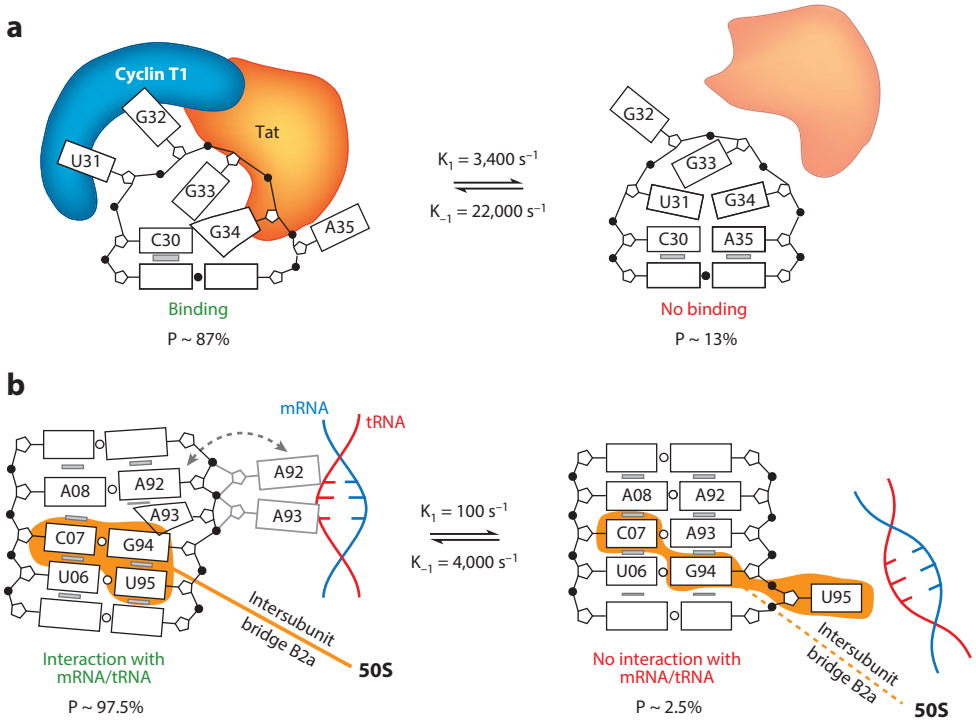

Figure 5

Functions of base-pair reshuffling dynamics. (*a*) In the apical loop of HIV-1 TAR (*trans*-activation response element), the minor conformational substate (CS) sequesters residues involved in HIV Tat and Cyclin T1 binding during transcriptional activation (55). (*b*) In the major CS of the ribosomal A-site, A1492 (A92) and A1493 (A93) are free to interact with and stabilize cognate messenger RNA–transfer RNA (mRNA–tRNA) minihelices during decoding, indicated by the gray dashed arrow and alternative A92/A93 conformation. The minor CS sequesters these residues, inhibiting decoding and disrupting the B2a intersubunit bridge (55).

regulatory switch. Similar pH-dependent base-pair reshuffling has also been observed near the catalytic active sites of the lead-dependent ribozyme (56, 61, 62) and spliceosome (57, 58) and may play an important role in catalysis.

For the ribosomal A-site, the higher-energy CS sequesters adenine residues that otherwise need to be free to carry out decoding functions (5; X. Zeng, J. Chugh, A. Casiano-Negroni, H.M. Al-Hashimi & C.L. Brooks III, manuscript submitted) and may play a role in processes that bypass decoding, such as frameshifting or stop-codon readthrough (**Figure 5*b***) (55). Interestingly, a conserved noncanonical motif in one of the helices of the purine riboswitch aptamer has been shown to tune ligand affinity and binding kinetics by altering the local pairing dynamics of the ligand-free state (64). More broadly, many internal and apical loops undergo rearrangements in their noncanonical pairs when participating in RNA–RNA tertiary interactions, suggesting that reshuffling dynamics may facilitate these molecular recognition events (65–72).

Base-Pair Isomerization

Overview. Two bases can often pair with each other in more than one configuration, representing different substates within a secondary structure. For example, G–U, G–G, A–A, and A–C base pairs, among others, can form in different arrangements that vary on the basis of glycosidic bond angle (*syn* versus *anti*), and sometimes protonation state, such as

for A–C base pairs (**Figure 3**) (73, 74). Similar to other base-pair dynamics, these different pairing forms can dynamically exchange on microsecond to millisecond timescales, or one form or another can be readily stabilized by environmental conditions (56, 75–79). These pairs can also involve rare tautomers (80), and in the case of DNA, even WC base pairs can transiently adopt Hoogsteen base pairs (59, 60). However, such WC Hoogsteen base pairs have yet to be reported in A-form RNA.

Biological significance. Isomerizations can significantly alter the chemical appearance of a base pair by exposing alternative functional groups to the major and minor grooves. They can also lead to more global changes in the 3D structure of a helix by altering backbone conformation. These structural changes can play important roles in mediating molecular recognition, as has been observed in binding of the Rev peptide to the HIV Rev response element (81), RNA tertiary interactions as in K-turn motifs (82), and specific ion binding in a group I intron (83). By changing the local steric profile of the base pair bordering a junction, these changes may also modulate the interhelical dynamics across junctions (see the section titled Interdependence of Substates Across Tiers, below) (50). Interestingly, tautomer-driven base-pair isomerizations affect ribosomal decoding (80, 84–86). A recent study reported that uridine tautomerization can allow a noncognate G–U base pair in the mRNA–tRNA minihelix to adopt a WC-like rather than wobble conformation, changing the profile of the base pair and circumventing the mechanism used by the ribosome to reject noncognate codons (80). Note, however, that the high free-energy cost of such tautomerizations ensures that decoding accuracy is not significantly compromised (63; X. Zeng, J. Chugh, A. Casiano-Negroni, H.M. Al-Hashimi & C.L. Brooks III, manuscript submitted). Alternatively, posttranscriptional chemical modifications of some tRNA anticodons appear to play an important role in decreasing the energetic cost of tautomerization, allowing the tRNA to form WC-like pairs with multiple different mRNA codons and thus to expand its decoding capacity (84–86).

Tertiary-Structure Dynamics

Overview. In many RNAs, distal loops form long-range tertiary contacts that are stabilized by canonical and noncanonical base-pairing, stacking, tightly bound cations, and weaker interactions involving base triples and A-minor motifs (87). Such tertiary interactions play critical roles in stabilizing the overall 3D structure of an RNA and in properly positioning key residues that form ligand binding and catalytic sites. The structural elements participating in tertiary interactions can undergo any one of the base-pair dynamic modes, including melting, reshuffling, and isomerization, which can result in the dynamic jittering of adjoined stems. In certain cases, these interactions can cooperatively melt, often precipitating large-amplitude interhelical dynamics that lead to global remodeling of 3D structure. Depending on the strength of these interactions, and the extent to which they are disrupted, such motions can occur at timescales ranging from microseconds to seconds.

In an increasing number of cases, tertiary-structure dynamics have been shown to be coupled to other motional modes in Tier 1. As mentioned above, many internal loops undergo reshuffling and melting dynamics following the formation of tertiary contacts. More dramatic couplings are also possible; a prototypical example is provided by the P5abc domain of the *Tetrahymena* group I ribozyme. Here, Mg^{2+}-induced folding of tertiary structure is coupled to reshuffling, entailing a 1-bp register shift of the P5c helix. This shift causes a loss of several G–U pairs but is more than offset by new local noncanonical and long-range tertiary pairs, as well as by Mg^{2+} interactions (**Figure 6*a***) (88). Recent molecular dynamics (MD) and experimental studies have shown that tertiary-structure formation and secondary-structure reorganization occur concomitantly, with a rate-limiting step that is independent of base-pair reshuffling (89).

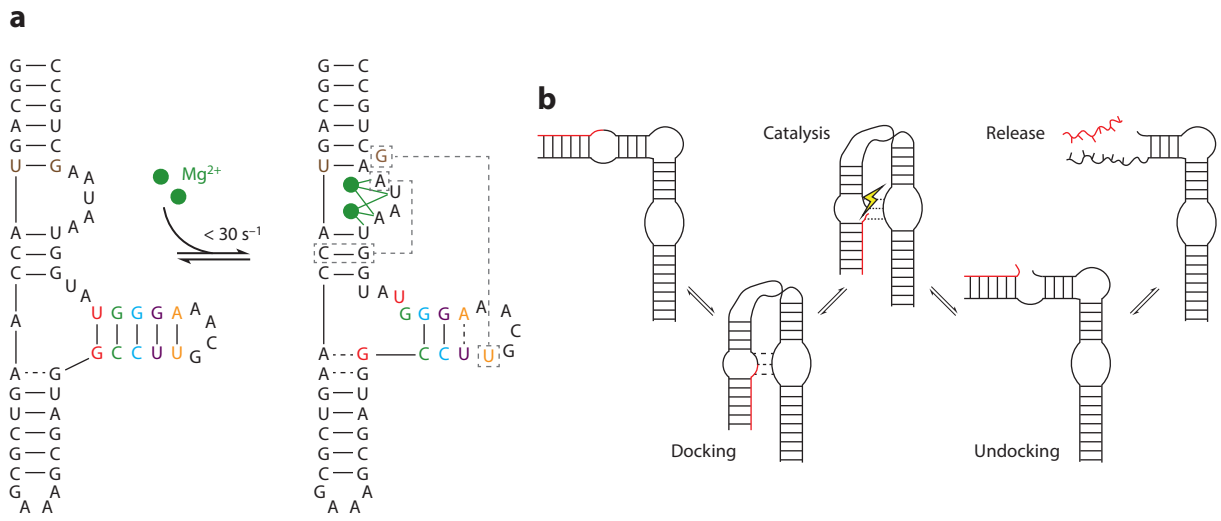

Figure 6

(*a*) Coupling of base-reshuffling and tertiary-structure dynamics in the P5abc domain of the *Tetrahymena thermophila* group I ribozyme. Following binding of two Mg^{2+} ions (183), the P5c stem (*colored*) undergoes a 1-nt register shift, releasing U168 to participate in a long-range pair (*right*, *boxed*). Additional tertiary interactions also form upon folding. NMR studies observed the two conformations to be in slow exchange (88), in agreement with data from recent stopped-flow experiments (89). Dashed lines indicate noncanonical pairs. (*b*) Enzymatic cycle of the hairpin ribozyme (92).

Biological significance. By both modulating access and remodeling the structure of binding and catalytic sites, tertiary-structure dynamics can serve many functions. For example, they play a prominent role in catalytic cycles of ribozymes, where they are used to achieve processivity and rapid turnover. In a common strategy, an undocked inactive conformation enables rapid substrate binding (90–92). The substrate then docks into the catalytic active site, where it is stabilized and aligned for catalysis by tertiary interactions (**Figure 6*b***). Following catalysis, melting of these tertiary interactions precipitates transitions back to the undocked state, where the product is efficiently released. In other catalytic RNAs, more local rearrangements (involving melting and reshuffling of active-site tertiary interactions) help drive substrate exchange and catalysis (93–96). In riboswitches, local tertiary melting dynamics, such as those observed in the pseudoknot of the ligand-bound preQ$_1$ riboswitch, may help facilitate fast ligand binding and/or unbinding, perhaps tuning switching activity (97).

In addition to facilitating switching between distinct functional states, tertiary dynamics can also toggle a molecule between active and inactive conformations, thereby tuning activity. In a unique example, a pH-dependent tertiary folding equilibrium involving formation of base triples between the pseudoknot loop and the pseudoknot helices of the *Murine leukemia virus* (MLV) readthrough element dictates the ratio of stop-codon readthrough during translation of the MLV mRNA (98). Thus, this equilibrium controls the cellular ratio of the proteins encoded upstream and downstream of the pseudoknot (98). In the *Tetrahymena* ribozyme, extremely long lived local tertiary-structure heterogeneties in the substrate binding site cause docking kinetics to vary by as much three orders of magnitude between individual molecules (99). These slow tertiary-structure dynamics, which may arise from differentially bound Mg^{2+} ions (100) and/or alternative sugar pucker conformations (101), do not alter the rate of single-turnover catalysis. However, they may play roles in other

aspects of ribozyme function by destabilizing the catalytically competent conformation.

Perhaps the most precise use of tertiary-structure dynamics involves those used by the ribosome during mRNA decoding (5, 8). During tRNA initial selection, tertiary-structure dynamics involving formation of A-minor interactions between the ribosomal A-site and the anticodon–codon minihelix stabilize cognate mRNA–tRNA pairs, preventing tRNA dissociation and driving domain-closure conformational changes of the ribosome that activate GTP hydrolysis in EF-Tu (**Figure 5*b***) (102–107; X. Zeng, J. Chugh, A. Casiano-Negroni, H.M. Al-Hashimi & C.L. Brooks III, manuscript submitted). Remarkably, a single incorrect base pair between the mRNA and tRNA is sufficient to disfavor these conformational changes, forming the basis for the 10^2–10^3-fold specificity for cognate tRNAs during initial selection (108). During the second kinetic proofreading step, a competition between the rates of tertiary-structure melting of the tRNA–mRNA minihelix and the rate of accommodation of the tRNA into the ribosome provides a further 10- to 100-fold specificity for cognate tRNAs, as noncognate tRNAs disassociate faster due to their weaker interactions with the A-site (106–109).

TIER 2: JITTERING DYNAMICS

Within the free-energy basin defined by a specific global secondary structure, local noncanonical pairing, and tertiary interactions, RNAs undergo a wide range of motions, including flipping in and out of unpaired bulge and internal loop residues, sugar repuckering, phosphate-backbone reorientations, and collective motions of helical domains. These motions cover timescales ranging from picoseconds to microseconds and can be loosely grouped into base-stacking and jittering dynamics. Base-stacking dynamics are the slower of the two, with timescales ranging from nanoseconds to microseconds, and involve transition states that require disruption of either interhelical stacking across an interhelical junction, stacking between an unpaired loop residue and a neighboring base pair, or stacking between two unpaired bases. The extent of these dynamics strongly depends on context; purine–purine stacks are much stronger and thus less dynamic than pyrimidine–pyrimidine stacks (110). Superimposed on these dynamics are faster, picosecond-to-nanosecond jittering dynamics, which can range from small-amplitude variations in local geometry of WC base pairs to much larger-amplitude motions in unstacked and flipped-out nucleobases. They can also involve variable-amplitude interhelical motions. Together, these Tier 2 motions span a wider range of timescales compared with Tiers 0 and 1; however, they are difficult to decompose into distinct tiers because the same type of motional mode (e.g., interhelical dynamics) can occur over the entire range of timescales and because these distinct motional modes often coexist and couple to one another.

Interhelical Dynamics

Overview. Together, local noncanonical pairs and global secondary structure define helical domains that are linked together by various flexible, single-stranded junctions. The relative orientation and translation of these helical domains play a central role in defining overall RNA architecture and the relative positioning of groups that participate in long-range tertiary interactions, catalytic activity, and protein binding (9, 111). In many RNAs, however, helices are not pinned down but rather undergo large collective motions that take place primarily at timescales ranging from nanoseconds to microseconds (**Figure 7*a***) (112–123). In some cases, such as in four-way junctions, these motions occur on slower timescales ranging from milliseconds to seconds (118); these slow timescales are probably due to strong cooperative stacking interactions that are unique to these junctions.

Interhelical dynamics have been studied in greatest detail in the 3-nt bulge of HIV-1 TAR. Various NMR and combined NMR–MD studies have revealed that these dynamics represent

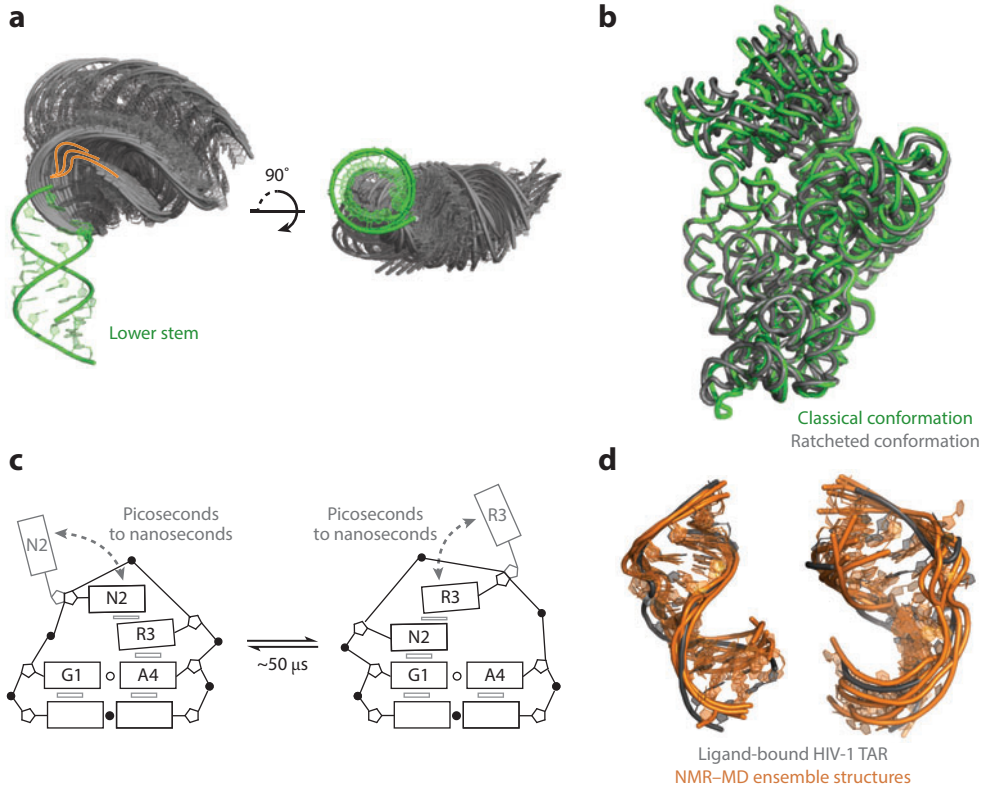

Figure 7

Modes and functions of Tier 2 jittering dynamics. (*a*) View of the 50 most probable interhelical conformations for a 3-nt two-helix bulge junction superimposed by the lower stem (*green*). The most probable conformations were obtained from coarse-grained model simulations that included only steric and connectivity forces (184). Bulge residues were included in coarse-grained modeling but are not shown here; rather, they are indicated by orange lines highlighting the possible paths of the bulge. (*b*) Superposition of classical (*green*) [Protein Data Bank (PDB) identifier 2WDG] and ratcheted EF-G bound 16S rRNA conformations (*gray*) (PDB 4JUW), highlighting the large interhelical dynamics associated with ribosomal translocation. In this view, H44 is vertical and facing the page. The two conformations were superimposed using residues 1,410–1,430 and 1,470–1,490 of H44. (*c*) Dynamics of the GNRA tetraloop observed by fluorescence spectroscopy (160). Exchange timescales correspond to rates measured by base (56) and sugar carbon (159) NMR relaxation dispersion experiments. (*d*) Superposition of ligand-bound HIV-1 TAR (*trans*-activation response element) structures (*gray*) with the five conformers from a high-resolution NMR–MD (molecular dynamics) ensemble that have the lowest heavy-atom root-mean-square deviation to the ligand-bound structures (*orange*) (124). (*Left*) PDB 1LVJ. (*Right*) PDB 1UTS.

a superposition of slower stacking and unstacking transitions on microsecond timescales, as well as faster nanosecond motions within the basin defined by a set of stacking interactions (112, 113, 124). Specifically, TAR interconverts between (*a*) a predominantly bent conformation that is stabilized by a stacking interaction between one of the bulge residues and the top of the lower helix and (*b*) a lower populated coaxially stacked conformation. On nanosecond timescales, the interhelical bend angle of the bent conformation fluctuates between 20° and 90°, whereas the stacked conformation samples only 0° to 20° bend angles (124). Raising the salt concentration, or mutations that increase the strength of interhelical stacking interactions, increases the population of the stacked conformation (125, 126). However, because stacking interactions usually provide no more than −3 kcal/mol in stabilizing

energy (127, 128), even strongly stacked junctions are likely to exist in unstacked conformations with approximately ≥1% populations.

An important and universal feature of interhelical dynamics is that the accessible helical orientations are strongly limited by steric and connectivity constraints, which together are referred to as topological constraints (**Figure 7*a***) (50, 111, 129, 130). These constraints are encoded at the secondary-structure and base-pair levels (Tiers 0 and 1) by the number of unpaired residues within the loops that connect a junction's helices. These constraints make it possible to construct RNA systems in which helical domains bend in a very directional manner, which can serve a diversity of functions.

Biological significance. Interhelical motions often enable RNAs to adapt their conformation to optimize intermolecular interactions with protein and ligand binding partners. For example, high-resolution structures of tRNA, tRNA–protein, and tRNA–ribosome complexes reveal that binding is often accompanied by significant changes in the relative orientation of tRNA's four helical domains (131). Similarly, the two helices of HIV-1 TAR adopt highly varied interhelical orientations when bound to different small molecules, corresponding to the interhelical conformations that are sampled in the absence of ligand (113, 124, 129, 132). In more complex RNAs, interhelical motions have been implicated in the ligand recognition processes of many riboswitch aptamer domains (133–139). Interestingly, cofactor-induced interhelical changes can also serve as transducers, triggering additional functional events. Specifically, successive changes in interhelical orientations induced by protein binding are thought to help order the assembly of complex ribonucleoprotein (RNP) machines, including the 30S ribosome (140, 141), the signal recognition particle (142), and telomerase (143).

The low energy barriers and directionality of interhelical motions also make them an ideal medium for executing the mechanical motions that underlie the processivity and turnover of ribozymes and RNPs, such as the ribosome and telomerase. Examples of some of these motions, such as docking and undocking of ribozyme substrates, are mentioned above. However, the most impressive are those demonstrated by the ribosome during tRNA translocation (**Figure 7*b***) (144, 145). Collectively referred to as ratcheting, these motions involve large, allosterically coupled changes in interhelical conformation of the 30S head and body domains and the 50S L1 stalk, as well as substantial distortions of the tRNA (146–151). These motions remove steric roadblocks to translocation and help transition the ribosome and tRNAs between different intermediates that are stabilized by alternative sets of tertiary interactions. For example, L1 stalk dynamics allow the stalk to form tertiary interactions with P-site tRNAs and then shuttle them to the E-site (152–154). Notably, early theoretical studies demonstrated that ratcheting is inherent to the gross architecture of the ribosome, consistent with a model in which the inherent flexibility of RNA junctions drives these rearrangements (151). The finding that the inhibitory effects of many antibiotics are derived in part from their ability to alter or arrest ribosomal ratcheting underscores the centrality of these collective motions to ribosome function (155–157).

Loop Dynamics

Overview. RNA secondary structure consists of A-form helical domains that are linked and capped by loops. These single-stranded regions of RNA structure often form important flexible sites for recognition of proteins, RNAs, ligands, and small molecules, and for formation of tertiary interactions. Adaptive changes in loop conformation helps optimize these intermolecular interactions, and in the absence of tertiary or ternary stabilizing interactions, these regions are among the most dynamic in RNA. Similar to interhelical dynamics, loop dynamics occur at timescales ranging from picoseconds to microseconds, corresponding to large-amplitude jittering dynamics of unstacked residues, smaller jittering of stacked

residues, and slower transitions involving exchange between alternatively stacked conformations. Such dynamics can cause isolated local changes in 3D structure or, for loops located in interhelical junctions, can drive global interhelical dynamics (112, 124).

Loop dynamics are well illustrated by the extensively studied GNRA tetraloop (**Figure 7*c***) (56, 158–163). Although the bookending guanine and adenine residues form a noncanonical Hoogsteen pair, which transiently melts on microsecond timescales, the middle N (any base) and R (purine) residues adopt a heterogeneous set of conformations that feature different stacking arrangements on top of the G–A pair that interconvert on microsecond timescales. In turn, the most solvent-exposed residue of each subconformation exhibits faster picosecond to nanosecond unstacking and jittering dynamics that, interestingly, appear to depend partly on the protonation states of the loop residues (164). A similar separation of timescales between the dynamics of paired and single-stranded loop residues has been observed for the dominant pairing state of the ribosomal A-site internal loop (**Figure 5*b***) (55; X. Zeng, J. Chugh, A. Casiano-Negroni, H.M. Al-Hashimi & C.L. Brooks III, manuscript submitted). In the absence of tRNA, the unpaired and weakly stacked A93 undergoes fast nanosecond motions as it moves in and out of the helical junction. In contrast, A92 forms a noncanonical pair with A08 and exhibits slower base-pair melting dynamics.

Biological significance. As mentioned above, the ability of unpaired residues to adopt alternative conformations with low energetic penalties is heavily utilized in RNA recognition processes, allowing the RNA loop to adapt to its molecular partner (165–167). In a recent interesting example, structural changes in an mRNA apical loop induced by binding of either of two proteins mediated the cooperative binding of the second protein to the same motif (168). In all of these cases, it is important to note that the observed adaptation corresponds to stabilization of preexisting low free-energy conformations. Notably, strongly stacked residues are unlikely to adopt unstacked conformations, as illustrated by the overwhelming propensity of GNRA tetraloops to adopt fully stacked conformations when participating in tertiary interactions (161). Likewise, studies of the apical loop and 3-nt bulge of HIV-1 TAR indicate that the various ligand-bound conformations of these regions strongly correlate with those that are sampled by TAR in the absence of ligand (**Figure 7*d***) (124, 132, 169). Thus, whether weakly stacked and highly dynamic or more strongly stacked and exhibiting only small local jittering, even at the highest level of the hierarchy the RNA free-energy landscape is tightly linked to function.

INTERDEPENDENCE OF SUBSTATES ACROSS TIERS

An interesting attribute of the RNA free-energy landscape and corresponding dynamics that is only beginning to be explored is the interdependence of CSs across different tiers. For example, a given secondary structure at Tier 0 may be able to form only a single set of tertiary interactions in Tier 1, thereby in a sense encoding the properties of Tier 1. Similarly, the number of different loop conformations along Tier 2 can influence the entropic cost associated with the formation of tertiary interactions along Tier 1. An exciting aspect of these interdependencies is that interactions that stabilize specific CSs in higher-order tiers can propagate into stabilization of specific CSs in lower tiers, which could increase the points of entry for effecting RNA conformational changes. Below, we discuss some of the better-understood dependencies and their potential connections to biological function. Although this is not the topic of this review, note that the coupling between tiers can be much more complex in the folding of large RNAs from unstructured states (170).

Secondary-Structure and Tertiary-Structure Dynamics

One of the most important interdependencies among tiers is that between tertiary and

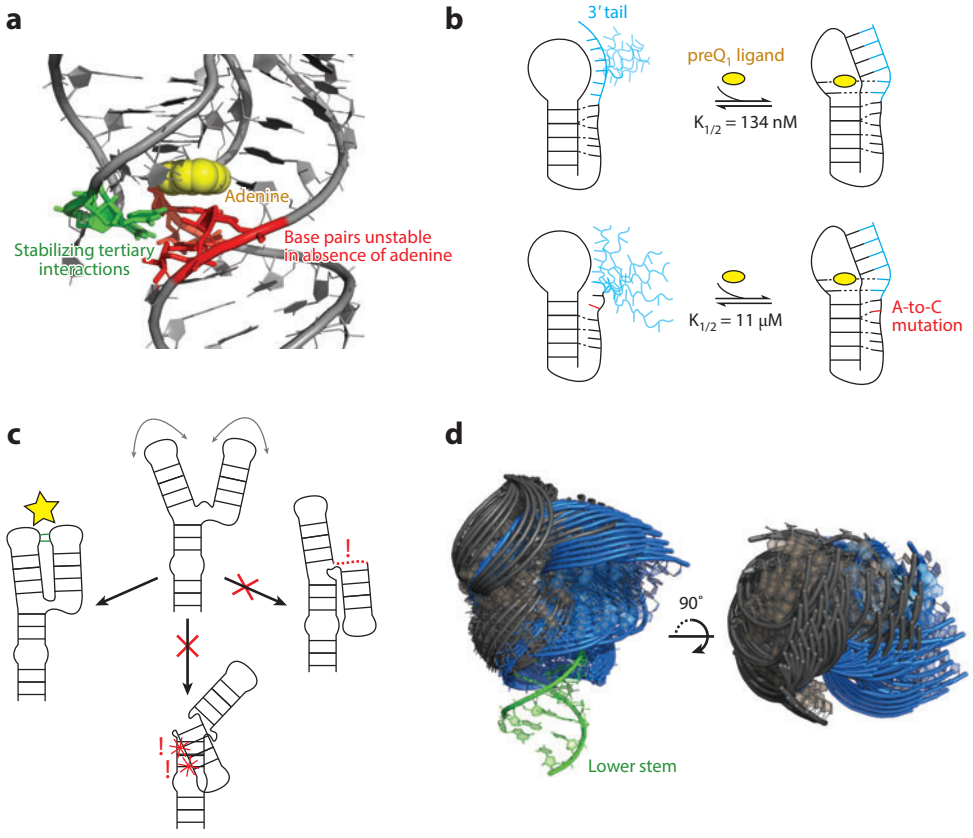

Figure 8

Interdependencies of conformational substates across tiers. (*a*) Aptamer domain of the *add* adenine riboswitch in complex with adenine (*yellow*) [Protein Data Bank (PDB) identifier 1Y26]. P1 stem base pairs that are unstable in the absence of ligand are colored red (31); J2/3 residues that provide stabilizing A-minor interactions are colored green. (*b*) Stacking interactions limit loop dynamics and preorganize the 3′ tail for ligand binding and pseudoknot folding in the wild-type *Bsu* preQ$_1$ riboswitch aptamer (*top*). An A-to-C mutation distal from the ligand binding pocket disrupts stacking, increasing dynamics and reducing ligand/riboswitch affinity (*bottom*) (177). The preQ$_1$ ligand, 3′ tail, and mutation are colored yellow, blue, and red, respectively. (*c*) Topological constraints preclude a theoretical three-way junction from forming two of three possible tertiary interactions. (*Right*) The interaction is precluded due to connectivity. (*Bottom*) The interaction is precluded due to sterics. (*d*) View of the 50 most probable interhelical conformations for two 1-nt bulge junctions superimposed by the lower stem (*green*). The bulge of the blue junction is located 2 bp below that of the gray junction. The most probable conformations were obtained from coarse-grained model simulations that included only steric and connectivity forces (184).

secondary structure, in which free energy supplied by tertiary interactions helps stabilize a secondary structure that would otherwise be unstable. Riboswitches provide the most important example of such interdependencies; ligand binding and subsequent formation of other tertiary interactions provide the necessary interaction energy to stabilize the functional secondary-structure switch either at equilibrium or transiently during cotranscriptional folding (**Figure 8*a***) (24, 29, 171). In other cases, proteins that stabilize RNA tertiary interactions can stabilize specific RNA secondary structures. For instance, coupled binding of the maturase and Mrs1 protein cofactors to the RNA of the bI3 group I intron stabilizes

native tertiary contacts, promoting reorganization of a nonnative intermediate secondary structure (172). Similar protein-induced secondary-structure rearrangements play important roles in ribosome assembly (173, 174).

Tertiary Structure and Loop Dynamics

Tertiary-structure dynamics involving the formation and melting of loop contacts are tightly linked to loop dynamics of the melted state. The extent of these loop dynamics, and their relative order or disorder, encodes an entropic penalty for folding. For example, the extensive loop dynamics of the single-stranded tRNA 3′ CCA have been suggested to play a critical role in resisting tRNA accommodation on the ribosome, a transition that involves the formation of several tertiary pairs between the 3′ CCA and the ribosome peptidyl transferase center (175). The entropic barrier presented by these dynamics helps order the accommodation process, preventing premature 3′ CCA entry and peptide transfer, and may also help tune accommodation kinetics, which is important for kinetic proofreading.

Another recent example involves the $preQ_1$ riboswitch aptamer. In this system, strong stacking interactions in the ligand-free state order the loop that folds around the $preQ_1$ ligand upon binding (**Figure 8*b***) (176, 177). Mutations that decrease stacking, and thus increase loop dynamics, significantly reduce ligand affinity.

Tertiary Structure and Interhelical Dynamics

As discussed above in the section titled Interhelical Dynamics, the basin of interhelical conformations defined by secondary structure can be quite limited. Emerging research has indicated that these limitations can directly affect tertiary-structure dynamics both by modulating the accessibility of the interhelical conformations needed to form a set of tertiary contacts and by modulating the entropy of the unfolded state (111). For example, theoretical research on a model two-helix junction has demonstrated that interhelical dynamics strongly discriminate against the formation of tertiary contacts between some helical faces but allow others (**Figure 8*c***) (130). Subsequent studies have suggested that this property of interhelical dynamics is broadly used by RNAs to encode their native folds (50, 129, 178, 184; A.M. Mustoe, H.M. Al-Hashimi & C.L. Brooks III. "Topological constraints are major determinants of tRNA tertiary structure and dynamics and provide basis for tertiary folding cooperativity," manuscript submitted). Importantly, such a strategy may explain how RNAs can overcome the limited information content of tertiary interactions, some of which (e.g., A-minor motifs) appear to have little sequence specificity (179, 180). Limited interhelical dynamics may also explain the ability of distal tertiary interactions to cooperatively stabilize each other, a property that is crucial to tertiary-structure stability (181, 182).

Base Reshuffling and Interhelical Dynamics

As mentioned above, alternative stacking conformations of single-stranded residues in a junction can favor distinct interhelical orientations. Base-reshuffling dynamics can have even greater effects by redefining junction topology and thereby driving even larger changes in interhelical orientation. Consider, for example, the ribosomal A-site RNA system. As noted above, the A-site internal loop exhibits base-reshuffling dynamics between two alternative local base-pairing CSs (**Figure 5*b***) (55). Both states effectively have a single bulged residue; however, in the dominant state, A93 is the bulge, whereas in the second, less energetically favorable state, the bulge migrates 2 bp down to U95. This migration of the bulge redirects the set of interhelical orientations that are topologically allowed, permitting sampling of certain interhelical orientations that would otherwise be inaccessible in the more energetically favorable pairing state (**Figure 8*d***). Similar topology-altering changes in local base-pairing induced by tertiary interactions or protein binding may also modify interhelical dynamics and affect

downstream behavior (50, 100). Alternatively, the number of interhelical conformations available to different CSs may influence base-pair reshuffling equilibria through entropic effects. Although such couplings are only beginning to be uncovered, we predict that they may be used by RNAs to transmit local changes in structure into larger-scale changes.

CONCLUSIONS

The past decade alone has witnessed an astounding explosion in the number of biological roles associated with RNA. Although the mechanisms of action and, indeed, functions of most of these RNAs remain to be elucidated, given our current understanding of RNA biology it is virtually assured that dynamics will prove to be a central component. As the complexity of the RNA functional universe increases, it will only become more important to establish a common framework for understanding recurrent dynamics strategies.

As discussed above, we suggest that RNA dynamics can be naturally classified in terms of transitions between basins on different tiers of a hierarchical free-energy landscape. This description, in turn, reveals that the same type of dynamics is often used to effect a particular kind of mechanism that can be wired into biological circuits to achieve diverse functional outcomes. Thus, secondary-structure transitions and base-pair dynamics can expose or sequester key functional elements, and jittering motions play a universal role in conformational adaptation and driving the motions that power RNA and RNP machines. Additional dynamic complexity can be achieved by coupling distinct motional modes, thereby presenting several points of entry for triggering a given type of overall dynamics. Despite the limitations of the above classification—it is not always possible to deconvolute dynamics within a single tier into individual motional modes, and the wide range of timescales covered by tertiary and secondary-structure dynamics can blur the distinction between the two—we hope that such an approach will help facilitate a more universal understanding of the link between RNA function and dynamics.

SUMMARY POINTS

1. RNA dynamics can be classified into different motional modes that occur on different tiers of a hierarchical free-energy landscape.
2. RNAs often harness multiple modes to achieve complex functionality.
3. Functional transitions occur primarily between preexisting favorable CSs of quiescent RNAs.
4. RNA dynamics may involve significant changes in structure, but these changes are directed to only a limited number of favorable substates.

FUTURE ISSUES

1. What are the physical basis and functional importance of the long-lived Mg^{2+}-dependent tertiary-structure heterogeneities that have been observed in several different nucleic acids?
2. How do environmental factors, such as metal ions and molecular crowders, influence the RNA free-energy landscape and the dynamic modes?

3. How important to RNA function are the interdependencies between different dynamics tiers?
4. Are there other motional modes that have yet to be discovered?

DISCLOSURE STATEMENT

H.M.A. is an advisor to and holds an ownership interest in Nymirum, Inc., which is an RNA-based drug-discovery company. The research reported in this review was performed by the University of Michigan faculty and students and was funded by National Institutes of Health and National Science Foundation contracts to H.M.A.

ACKNOWLEDGMENTS

We thank Isaac Kimsey for his input and assistance in the preparation of figures, and Shan Yang and Dr. Yi Xue for their comments. H.M.A. gratefully acknowledges the Michigan Economic Development Cooperation and the Michigan Technology Tri-Corridor for their support in the purchase of a 600-MHz spectrometer. Our research is supported by the National Institutes of Health (R01 AI066975, R01 GM089846, P01 GM0066275, and NIAID R21 AI096985 to H.M.A.; R21 GM096156 to C.L.B. and H.M.A; RR012255 to C.L.B.) and the National Science Foundation (Graduate Research Fellowship to A.M.M., Career Award CHE0918817 to H.M.A., PHY0216576 to C.L.B.).

LITERATURE CITED

1. Kruger K, Grabowski PJ, Zaug AJ, Sands J, Gottschling DE, Cech TR. 1982. Self-splicing RNA: auto-excision and autocyclization of the ribosomal RNA intervening sequence of *Tetrahymena*. *Cell* 31:147–57
2. Guerrier-Takada C, Gardiner K, Marsh T, Pace N, Altman S. 1983. The RNA moiety of ribonuclease P is the catalytic subunit of the enzyme. *Cell* 35:849–57
3. Serganov A, Patel DJ. 2012. Metabolite recognition principles and molecular mechanisms underlying riboswitch function. *Annu. Rev. Biophys.* 41:343–70
4. Reiter NJ, Chan CW, Mondragon A. 2011. Emerging structural themes in large RNA molecules. *Curr. Opin. Struct. Biol.* 21:319–26
5. Voorhees RM, Ramakrishnan V. 2013. Structural basis of the translational elongation cycle. *Annu. Rev. Biochem.* 82:203–36
6. Djebali S, Davis CA, Merkel A, Dobin A, Lassmann T, et al. 2012. Landscape of transcription in human cells. *Nature* 489:101–8
7. Bernstein BE, Birney E, Dunham I, Green ED, Gunter C, Snyder M. 2012. An integrated encyclopedia of DNA elements in the human genome. *Nature* 489:57–74
8. Zaher HS, Green R. 2009. Fidelity at the molecular level: lessons from protein synthesis. *Cell* 136:746–62
9. Cruz JA, Westhof E. 2009. The dynamic landscapes of RNA architecture. *Cell* 136:604–9
10. Dethoff EA, Chugh J, Mustoe AM, Al-Hashimi HM. 2012. Functional complexity and regulation through RNA dynamics. *Nature* 482:322–30
11. Frauenfelder H, Sligar SG, Wolynes PG. 1991. The energy landscapes and motions of proteins. *Science* 254:1598–603
12. Tinoco I Jr, Bustamante C. 1999. How RNA folds. *J. Mol. Biol.* 293:271–81
13. Brion P, Westhof E. 1997. Hierarchy and dynamics of RNA folding. *Annu. Rev. Biophys. Biomol. Struct.* 26:113–37

14. Ding Y, Lawrence CE. 2003. A statistical sampling algorithm for RNA secondary structure prediction. *Nucleic Acids Res.* 31:7280–301
15. McCaskill JS. 1990. The equilibrium partition function and base pair binding probabilities for RNA secondary structure. *Biopolymers* 29:1105–19
16. Wuchty S, Fontana W, Hofacker IL, Schuster P. 1999. Complete suboptimal folding of RNA and the stability of secondary structures. *Biopolymers* 49:145–65
17. Uhlenbeck OC. 1995. Keeping RNA happy. *RNA* 1:4–6
18. Treiber DK, Williamson JR. 2001. Beyond kinetic traps in RNA folding. *Curr. Opin. Struct. Biol.* 11:309–14
19. Fürtig B, Wenter P, Reymond L, Richter C, Pitsch S, Schwalbe H. 2007. Conformational dynamics of bistable RNAs studied by time-resolved NMR spectroscopy. *J. Am. Chem. Soc.* 129:16222–29
20. Xu X, Chen S-J. 2012. Kinetic mechanism of conformational switch between bistable RNA hairpins. *J. Am. Chem. Soc.* 134:12499–507
21. Grohman JK, Gorelick RJ, Lickwar CR, Lieb JD, Bower BD, et al. 2013. A guanosine-centric mechanism for RNA chaperone function. *Science* 340:190–95
22. Herschlag D. 1995. RNA chaperones and the RNA folding problem. *J. Biol. Chem.* 270:20871–74
23. Thirumalai D, Woodson SA. 1996. Kinetics of folding of proteins and RNA. *Acc. Chem. Res.* 29:433–39
24. Breaker RR. 2012. Riboswitches and the RNA world. *Cold Spring Harb. Perspect. Biol.* 4:a003566
25. Winkler W, Nahvi A, Breaker RR. 2002. Thiamine derivatives bind messenger RNAs directly to regulate bacterial gene expression. *Nature* 419:952–56
26. Caron MP, Bastet L, Lussier A, Simoneau-Roy M, Masse E, Lafontaine DA. 2012. Dual-acting riboswitch control of translation initiation and mRNA decay. *Proc. Natl. Acad. Sci. USA* 109:E3444–53
27. Cheah MT, Wachter A, Sudarsan N, Breaker RR. 2007. Control of alternative RNA splicing and gene expression by eukaryotic riboswitches. *Nature* 447:497–500
28. Mironov AS, Gusarov I, Rafikov R, Lopez LE, Shatalin K, et al. 2002. Sensing small molecules by nascent RNA: a mechanism to control transcription in bacteria. *Cell* 111:747–56
29. Haller A, Soulière MF, Micura R. 2011. The dynamic nature of RNA as key to understanding riboswitch mechanisms. *Acc. Chem. Res.* 44:1339–48
30. Kortmann J, Sczodrok S, Rinnenthal J, Schwalbe H, Narberhaus F. 2011. Translation on demand by a simple RNA-based thermosensor. *Nucleic Acids Res.* 39:2855–68
31. Reining A, Nozinovic S, Schlepckow K, Buhr F, Fürtig B, Schwalbe H. 2013. Three-state mechanism couples ligand and temperature sensing in riboswitches. *Nature* 499:355–59
32. Giuliodori AM, Di Pietro F, Marzi S, Masquida B, Wagner R, et al. 2010. The cspA mRNA is a thermosensor that modulates translation of the cold-shock protein CspA. *Mol. Cell* 37:21–33
33. Cromie MJ, Shi Y, Latifi T, Groisman EA. 2006. An RNA sensor for intracellular Mg^{2+}. *Cell* 125:71–84
34. Nechooshtan G, Elgrably-Weiss M, Sheaffer A, Westhof E, Altuvia S. 2009. A pH-responsive riboregulator. *Genes Dev.* 23:2650–62
35. Babitzke P, Yanofsky C. 1993. Reconstitution of *Bacillus subtilis* trp attenuation in vitro with TRAP, the trp RNA-binding attenuation protein. *Proc. Natl. Acad. Sci. USA* 90:133–37
36. Grundy FJ, Winkler WC, Henkin TM. 2002. tRNA-mediated transcription antitermination in vitro: codon–anticodon pairing independent of the ribosome. *Proc. Natl. Acad. Sci. USA* 99:11121–26
37. Vogel J, Luisi BF. 2011. Hfq and its constellation of RNA. *Nat. Rev. Microbiol.* 9:578–89
38. Semlow DR, Staley JP. 2012. Staying on message: ensuring fidelity in pre-mRNA splicing. *Trends Biochem. Sci.* 37:263–73
39. Huthoff H, Berkhout B. 2001. Two alternating structures of the HIV-1 leader RNA. *RNA* 7:143–57
40. Lu K, Heng X, Summers MF. 2011. Structural determinants and mechanism of HIV-1 genome packaging. *J. Mol. Biol.* 410:609–33
41. Lu K, Heng X, Garyu L, Monti S, Garcia EL, et al. 2011. NMR detection of structures in the HIV-1 5′-leader RNA that regulate genome packaging. *Science* 334:242–45
42. Snoussi K, Leroy JL. 2001. Imino proton exchange and base-pair kinetics in RNA duplexes. *Biochemistry* 40:8898–904
43. Chen C, Jiang L, Michalczyk R, Russu IM. 2006. Structural energetics and base-pair opening dynamics in sarcin–ricin domain RNA. *Biochemistry* 45:13606–13

44. Rinnenthal J, Klinkert B, Narberhaus F, Schwalbe H. 2010. Direct observation of the temperature-induced melting process of the *Salmonella* fourU RNA thermometer at base-pair resolution. *Nucleic Acids Res.* 38:3834–47
45. Woodson SA. 2010. Taming free energy landscapes with RNA chaperones. *RNA Biol.* 7:677–86
46. Jankowsky E. 2011. RNA helicases at work: binding and rearranging. *Trends Biochem. Sci.* 36:19–29
47. Shankar N, Xia T, Kennedy SD, Krugh TR, Mathews DH, Turner DH. 2007. NMR reveals the absence of hydrogen bonding in adjacent UU and AG mismatches in an isolated internal loop from ribosomal RNA. *Biochemistry* 46:12665–78
48. Conn GL, Draper DE, Lattman EE, Gittis AG. 1999. Crystal structure of a conserved ribosomal protein–RNA complex. *Science* 284:1171–74
49. Wang Y-X, Huang S, Draper DE. 1996. Structure of a U–U pair within a conserved ribosomal RNA hairpin. *Nucleic Acids Res.* 24:2666–72
50. Mustoe AM, Bailor MH, Teixeira RM, Brooks CL III, Al-Hashimi HM. 2012. New insights into the fundamental role of topological constraints as a determinant of two-way junction conformation. *Nucleic Acids Res.* 40:892–904
51. Schmeing TM, Huang KS, Strobel SA, Steitz TA. 2005. An induced-fit mechanism to promote peptide bond formation and exclude hydrolysis of peptidyl-tRNA. *Nature* 438:520–24
52. Qu X, Wen JD, Lancaster L, Noller HF, Bustamante C, Tinoco I Jr. 2011. The ribosome uses two active mechanisms to unwind messenger RNA during translation. *Nature* 475:118–21
53. Watts JM, Dang KK, Gorelick RJ, Leonard CW, Bess JW Jr, et al. 2009. Architecture and secondary structure of an entire HIV-1 RNA genome. *Nature* 460:711–16
54. Mouzakis KD, Lang AL, Vander Meulen KA, Easterday PD, Butcher SE. 2013. HIV-1 frameshift efficiency is primarily determined by the stability of base pairs positioned at the mRNA entrance channel of the ribosome. *Nucleic Acids Res.* 41:1901–13
55. Dethoff EA, Petzold K, Chugh J, Casiano-Negroni A, Al-Hashimi HM. 2012. Visualizing transient low-populated structures of RNA. *Nature* 491:724–28
56. Hoogstraten CG, Wank JR, Pardi A. 2000. Active site dynamics in the lead-dependent ribozyme. *Biochemistry* 39:9951–58
57. Venditti V, Clos L 2nd, Niccolai N, Butcher SE. 2009. Minimum-energy path for a U6 RNA conformational change involving protonation, base-pair rearrangement and base flipping. *J. Mol. Biol.* 391:894–905
58. Reiter NJ, Blad H, Abildgaard F, Butcher SE. 2004. Dynamics in the U6 RNA intramolecular stem-loop: a base flipping conformational change. *Biochemistry* 43:13739–47
59. Nikolova EN, Kim E, Wise AA, O'Brien PJ, Andricioaei I, Al-Hashimi HM. 2011. Transient Hoogsteen base pairs in canonical duplex DNA. *Nature* 470:498–502
60. Nikolova EN, Goh GB, Brooks CL III, Al-Hashimi HM. 2013. Characterizing the protonation state of cytosine in transient G • C Hoogsteen base pairs in duplex DNA. *J. Am. Chem. Soc.* 135:6766–69
61. Yajima R, Proctor DJ, Kierzek R, Kierzek E, Bevilacqua PC. 2007. A conformationally restricted guanosine analog reveals the catalytic relevance of three structures of an RNA enzyme. *Chem. Biol.* 14:23–30
62. Kadakkuzha BM, Zhao L, Xia T. 2009. Conformational distribution and ultrafast base dynamics of leadzyme. *Biochemistry* 48:3807–9
63. Manickam N, Nag N, Abbasi A, Patel K, Farabaugh PJ. 2014. Studies of translational misreading in vivo show that the ribosome very efficiently discriminates against most potential errors. *RNA* 20:9–15
64. Stoddard CD, Widmann J, Trausch JJ, Marcano-Velázquez JG, Knight R, Batey RT. 2013. Nucleotides adjacent to the ligand-binding pocket are linked to activity tuning in the purine riboswitch. *J. Mol. Biol.* 425:1596–611
65. Butcher SE, Dieckmann T, Feigon J. 1997. Solution structure of a GAAA tetraloop receptor RNA. *EMBO J.* 16:7490–99
66. Shankar N, Kennedy SD, Chen G, Krugh TR, Turner DH. 2006. The NMR structure of an internal loop from 23S ribosomal RNA differs from its structure in crystals of 50S ribosomal subunits. *Biochemistry* 45:11776–89
67. Schroeder SJ, Fountain MA, Kennedy SD, Lukavsky PJ, Puglisi JD, et al. 2003. Thermodynamic stability and structural features of the J4/5 loop in a *Pneumocystis carinii* group I intron. *Biochemistry* 42:14184–96

68. Rupert PB, Ferre-D'Amare AR. 2001. Crystal structure of a hairpin ribozyme–inhibitor complex with implications for catalysis. *Nature* 410:780–86
69. Butcher SE, Allain FH, Feigon J. 1999. Solution structure of the loop B domain from the hairpin ribozyme. *Nat. Struct. Biol.* 6:212–16
70. Cai Z, Tinoco I Jr. 1996. Solution structure of loop A from the hairpin ribozyme from tobacco ringspot virus satellite. *Biochemistry* 35:6026–36
71. Cate JH, Gooding AR, Podell E, Zhou K, Golden BL, et al. 1996. Crystal structure of a group I ribozyme domain: principles of RNA packing. *Science* 273:1678–85
72. Lee JC, Gutell RR, Russell R. 2006. The UAA/GAN internal loop motif: a new RNA structural element that forms a cross-strand AAA stack and long-range tertiary interactions. *J. Mol. Biol.* 360:978–88
73. Davis AR, Kirkpatrick CC, Znosko BM. 2011. Structural characterization of naturally occurring RNA single mismatches. *Nucleic Acids Res.* 39:1081–94
74. Leontis NB, Stombaugh J, Westhof E. 2002. The non–Watson–Crick base pairs and their associated isostericity matrices. *Nucleic Acids Res.* 30:3497–531
75. Gao XL, Patel DJ. 1988. $G_{Syn} \cdot A_{Anti}$ mismatch formation in DNA dodecamers at acidic pH; pH-dependent conformational transition of G·A mispairs detected by proton NMR. *J. Am. Chem. Soc.* 110:5178–82
76. Burkard ME, Turner DH. 2000. NMR structures of $r(GCA\underline{G}\underline{G}C\underline{G}UGC)_2$ and determinants of stability for single guanosine–guanosine base pairs. *Biochemistry* 39:11748–62
77. Yildirim I, Park H, Disney MD, Schatz GC. 2013. A dynamic structural model of expanded RNA CAG repeats: a refined X-ray structure and computational investigations using molecular dynamics and umbrella sampling simulations. *J. Am. Chem. Soc.* 135:3528–38
78. Chen G, Kennedy SD, Qiao J, Krugh TR, Turner DH. 2006. An alternating sheared AA pair and elements of stability for a single sheared purine–purine pair flanked by sheared GA pairs in RNA. *Biochemistry* 45:6889–903
79. Mathews DH, Case DA. 2006. Nudged elastic band calculation of minimal energy paths for the conformational change of a GG non-canonical pair. *J. Mol. Biol.* 357:1683–93
80. Demeshkina N, Jenner L, Westhof E, Yusupov M, Yusupova G. 2012. A new understanding of the decoding principle on the ribosome. *Nature* 484:256–59
81. Peterson RD, Feigon J. 1996. Structural change in Rev responsive element RNA of HIV-1 on binding Rev peptide. *J. Mol. Biol.* 264:863–77
82. Schroeder KT, Lilley DM. 2009. Ion-induced folding of a kink turn that departs from the conventional sequence. *Nucleic Acids Res.* 37:7281–89
83. Znosko BM, Kennedy SD, Wille PC, Krugh TR, Turner DH. 2004. Structural features and thermodynamics of the J4/5 loop from the *Candida albicans* and *Candida dubliniensis* group I introns. *Biochemistry* 43:15822–37
84. Weixlbaumer A, Murphy FV 4th, Dziergowska A, Malkiewicz A, Vendeix FA, et al. 2007. Mechanism for expanding the decoding capacity of transfer RNAs by modification of uridines. *Nat. Struct. Mol. Biol.* 14:498–502
85. Vendeix FA, Murphy FV 4th, Cantara WA, Leszczynska G, Gustilo EM, et al. 2012. Human $tRNA^{Lys3}_{UUU}$ is pre-structured by natural modifications for cognate and wobble codon binding through keto–enol tautomerism. *J. Mol. Biol.* 416:467–85
86. Cantara WA, Murphy FV 4th, Demirci H, Agris PF. 2013. Expanded use of sense codons is regulated by modified cytidines in tRNA. *Proc. Natl. Acad. Sci. USA* 110:10964–69
87. Butcher SE, Pyle AM. 2011. The molecular interactions that stabilize RNA tertiary structure: RNA motifs, patterns, and networks. *Acc. Chem. Res.* 44:1302–11
88. Wu M, Tinoco I Jr. 1998. RNA folding causes secondary structure rearrangement. *Proc. Natl. Acad. Sci. USA* 95:11555–60
89. Koculi E, Cho SS, Desai R, Thirumalai D, Woodson SA. 2012. Folding path of P5abc RNA involves direct coupling of secondary and tertiary structures. *Nucleic Acids Res.* 40:8011–20
90. Herschlag D. 1992. Evidence for processivity and two-step binding of the RNA substrate from studies of J1/2 mutants of the *Tetrahymena* ribozyme. *Biochemistry* 31:1386–99

91. Bevilacqua PC, Kierzek R, Johnson KA, Turner DH. 1992. Dynamics of ribozyme binding of substrate revealed by fluorescence-detected stopped-flow methods. *Science* 258:1355–58
92. Zhuang X, Kim H, Pereira MJ, Babcock HP, Walter NG, Chu S. 2002. Correlating structural dynamics and function in single ribozyme molecules. *Science* 296:1473–76
93. Marcia M, Pyle AM. 2012. Visualizing group II intron catalysis through the stages of splicing. *Cell* 151:497–507
94. Harris DA, Rueda D, Walter NG. 2002. Local conformational changes in the catalytic core of the *trans*-acting hepatitis delta virus ribozyme accompany catalysis. *Biochemistry* 41:12051–61
95. Lee TS, Giambasu G, Harris ME, York DM. 2011. Characterization of the structure and dynamics of the HDV ribozyme at different stages along the reaction path. *J. Phys. Chem. Lett.* 2:2538–43
96. Ke A, Zhou K, Ding F, Cate JH, Doudna JA. 2004. A conformational switch controls hepatitis delta virus ribozyme catalysis. *Nature* 429:201–5
97. Zhang Q, Kang M, Peterson RD, Feigon J. 2011. Comparison of solution and crystal structures of preQ$_1$ riboswitch reveals calcium-induced changes in conformation and dynamics. *J. Am. Chem. Soc.* 133:5190–93
98. Houck-Loomis B, Durney MA, Salguero C, Shankar N, Nagle JM, et al. 2011. An equilibrium-dependent retroviral mRNA switch regulates translational recoding. *Nature* 480:561–64
99. Solomatin SV, Greenfeld M, Chu S, Herschlag D. 2010. Multiple native states reveal persistent ruggedness of an RNA folding landscape. *Nature* 463:681–84
100. Hyeon C, Lee J, Yoon J, Hohng S, Thirumalai D. 2012. Hidden complexity in the isomerization dynamics of Holliday junctions. *Nat. Chem.* 4:907–14
101. Mortimer SA, Weeks KM. 2009. C2′-endo nucleotides as molecular timers suggested by the folding of an RNA domain. *Proc. Natl. Acad. Sci. USA* 106:15622–27
102. Ogle JM, Murphy FV 4th, Tarry MJ, Ramakrishnan V. 2002. Selection of tRNA by the ribosome requires a transition from an open to a closed form. *Cell* 111:721–32
103. Ogle JM, Brodersen DE, Clemons WM Jr, Tarry MJ, Carter AP, Ramakrishnan V. 2001. Recognition of cognate transfer RNA by the 30S ribosomal subunit. *Science* 292:897–902
104. Fourmy D, Recht MI, Blanchard SC, Puglisi JD. 1996. Structure of the A site of *Escherichia coli* 16S ribosomal RNA complexed with an aminoglycoside antibiotic. *Science* 274:1367–71
105. Schmeing TM, Voorhees RM, Kelley AC, Gao YG, Murphy FV 4th, et al. 2009. The crystal structure of the ribosome bound to EF-Tu and aminoacyl-tRNA. *Science* 326:688–94
106. Geggier P, Dave R, Feldman MB, Terry DS, Altman RB, et al. 2010. Conformational sampling of aminoacyl-tRNA during selection on the bacterial ribosome. *J. Mol. Biol.* 399:576–95
107. Blanchard SC, Gonzalez RL, Kim HD, Chu S, Puglisi JD. 2004. tRNA selection and kinetic proofreading in translation. *Nat. Struct. Mol. Biol.* 11:1008–14
108. Gromadski KB, Daviter T, Rodnina MV. 2006. A uniform response to mismatches in codon–anticodon complexes ensures ribosomal fidelity. *Mol. Cell* 21:369–77
109. Pape T, Wintermeyer W, Rodnina M. 1999. Induced fit in initial selection and proofreading of aminoacyl-tRNA on the ribosome. *EMBO J.* 18:3800–7
110. Turner DH, Sugimoto N, Freier SM. 1988. RNA structure prediction. *Annu. Rev. Biophys. Biophys. Chem.* 17:167–92
111. Bailor MH, Mustoe AM, Brooks CL III, Al-Hashimi HM. 2011. Topological constraints: using RNA secondary structure to model 3D conformation, folding pathways, and dynamic adaptation. *Curr. Opin. Struct. Biol.* 21:296–305
112. Zhang Q, Sun X, Watt ED, Al-Hashimi HM. 2006. Resolving the motional modes that code for RNA adaptation. *Science* 311:653–56
113. Zhang Q, Stelzer AC, Fisher CK, Al-Hashimi HM. 2007. Visualizing spatially correlated dynamics that directs RNA conformational transitions. *Nature* 450:1263–67
114. Sun X, Zhang Q, Al-Hashimi HM. 2007. Resolving fast and slow motions in the internal loop containing stem-loop 1 of HIV-1 that are modulated by Mg^{2+} binding: role in the kissing-duplex structural transition. *Nucleic Acids Res.* 35:1698–713

115. Bailor MH, Musselman C, Hansen AL, Gulati K, Patel DJ, Al-Hashimi HM. 2007. Characterizing the relative orientation and dynamics of RNA A-form helices using NMR residual dipolar couplings. *Nat. Protoc.* 2:1536–46
116. Getz MM, Andrews AJ, Fierke CA, Al-Hashimi HM. 2007. Structural plasticity and Mg^{2+} binding properties of RNase P P_4 from combined analysis of NMR residual dipolar couplings and motionally decoupled spin relaxation. *RNA* 13:251–66
117. Olsen GL, Bardaro MF Jr, Echodu DC, Drobny GP, Varani G. 2010. Intermediate rate atomic trajectories of RNA by solid-state NMR spectroscopy. *J. Am. Chem. Soc.* 132:303–8
118. Hohng S, Wilson TJ, Tan E, Clegg RM, Lilley DM, Ha T. 2004. Conformational flexibility of four-way junctions in RNA. *J. Mol. Biol.* 336:69–79
119. Melcher SE, Wilson TJ, Lilley DM. 2003. The dynamic nature of the four-way junction of the hepatitis C virus IRES. *RNA* 9:809–20
120. Reblova K, Sponer J, Lankas F. 2012. Structure and mechanical properties of the ribosomal L1 stalk three-way junction. *Nucleic Acids Res.* 40:6290–303
121. Besseova I, Reblova K, Leontis NB, Sponer J. 2010. Molecular dynamics simulations suggest that RNA three-way junctions can act as flexible RNA structural elements in the ribosome. *Nucleic Acids Res.* 38:6247–64
122. Grant GP, Boyd N, Herschlag D, Qin PZ. 2009. Motions of the substrate recognition duplex in a group I intron assessed by site-directed spin labeling. *J. Am. Chem. Soc.* 131:3136–37
123. Zhang Q, Kim NK, Peterson RD, Wang Z, Feigon J. 2010. Structurally conserved five nucleotide bulge determines the overall topology of the core domain of human telomerase RNA. *Proc. Natl. Acad. Sci. USA* 107:18761–68
124. Salmon L, Bascom G, Andricioaei I, Al-Hashimi HM. 2013. A general method for constructing atomic-resolution RNA ensembles using NMR residual dipolar couplings: the basis for interhelical motions revealed. *J. Am. Chem. Soc.* 135:5457–66
125. Stelzer AC, Kratz JD, Zhang Q, Al-Hashimi HM. 2010. RNA dynamics by design: biasing ensembles towards the ligand-bound state. *Angew. Chem. Int. Ed. Engl.* 49:5731–33
126. Casiano-Negroni A, Sun X, Al-Hashimi HM. 2007. Probing Na^{+}-induced changes in the HIV-1 TAR conformational dynamics using NMR residual dipolar couplings: new insights into the role of counterions and electrostatic interactions in adaptive recognition. *Biochemistry* 46:6525–35
127. Walter AE, Turner DH, Kim J, Lyttle MH, Müller P, et al. 1994. Coaxial stacking of helixes enhances binding of oligoribonucleotides and improves predictions of RNA folding. *Proc. Natl. Acad. Sci. USA* 91:9218–22
128. Tyagi R, Mathews DH. 2007. Predicting helical coaxial stacking in RNA multibranch loops. *RNA* 13:939–51
129. Bailor MH, Sun X, Al-Hashimi HM. 2010. Topology links RNA secondary structure with global conformation, dynamics, and adaptation. *Science* 327:202–6
130. Chu VB, Lipfert J, Bai Y, Pande VS, Doniach S, Herschlag D. 2009. Do conformational biases of simple helical junctions influence RNA folding stability and specificity? *RNA* 15:2195–205
131. Alexander RW, Eargle J, Luthey-Schulten Z. 2010. Experimental and computational determination of tRNA dynamics. *FEBS Lett.* 584:376–86
132. Frank AT, Stelzer AC, Al-Hashimi HM, Andricioaei I. 2009. Constructing RNA dynamical ensembles by combining MD and motionally decoupled NMR RDCs: new insights into RNA dynamics and adaptive ligand recognition. *Nucleic Acids Res.* 37:3670–79
133. Heppell B, Blouin S, Dussault AM, Mulhbacher J, Ennifar E, et al. 2011. Molecular insights into the ligand-controlled organization of the SAM-I riboswitch. *Nat. Chem. Biol.* 7:384–92
134. Haller A, Altman RB, Soulière MF, Blanchard SC, Micura R. 2013. Folding and ligand recognition of the TPP riboswitch aptamer at single-molecule resolution. *Proc. Natl. Acad. Sci. USA* 110:4188–93
135. Fiegland LR, Garst AD, Batey RT, Nesbitt DJ. 2012. Single-molecule studies of the lysine riboswitch reveal effector-dependent conformational dynamics of the aptamer domain. *Biochemistry* 51:9223–33
136. Stoddard CD, Montange RK, Hennelly SP, Rambo RP, Sanbonmatsu KY, Batey RT. 2010. Free state conformational sampling of the SAM-I riboswitch aptamer domain. *Structure* 18:787–97

137. Baird NJ, Ferre-D'Amare AR. 2010. Idiosyncratically tuned switching behavior of riboswitch aptamer domains revealed by comparative small-angle X-ray scattering analysis. *RNA* 16:598–609
138. Brenner MD, Scanlan MS, Nahas MK, Ha T, Silverman SK. 2010. Multivector fluorescence analysis of the *xpt* guanine riboswitch aptamer domain and the conformational role of guanine. *Biochemistry* 49:1596–605
139. Lipfert J, Das R, Chu VB, Kudaravalli M, Boyd N, et al. 2007. Structural transitions and thermodynamics of a glycine-dependent riboswitch from *Vibrio cholerae*. *J. Mol. Biol.* 365:1393–406
140. Mulder AM, Yoshioka C, Beck AH, Bunner AE, Milligan RA, et al. 2010. Visualizing ribosome biogenesis: parallel assembly pathways for the 30S subunit. *Science* 330:673–77
141. Adilakshmi T, Bellur DL, Woodson SA. 2008. Concurrent nucleation of 16S folding and induced fit in 30S ribosome assembly. *Nature* 455:1268–72
142. Menichelli E, Isel C, Oubridge C, Nagai K. 2007. Protein-induced conformational changes of RNA during the assembly of human signal recognition particle. *J. Mol. Biol.* 367:187–203
143. Stone MD, Mihalusova M, O'Connor CM, Prathapam R, Collins K, Zhuang X. 2007. Stepwise protein-mediated RNA folding directs assembly of telomerase ribonucleoprotein. *Nature* 446:458–61
144. Chen J, Tsai A, O'Leary SE, Petrov A, Puglisi JD. 2012. Unraveling the dynamics of ribosome translocation. *Curr. Opin. Struct. Biol.* 22:804–14
145. Frank J, Gonzalez RL Jr. 2010. Structure and dynamics of a processive Brownian motor: the translating ribosome. *Annu. Rev. Biochem.* 79:381–412
146. Ratje AH, Loerke J, Mikolajka A, Brunner M, Hildebrand PW, et al. 2010. Head swivel on the ribosome facilitates translocation by means of intra-subunit tRNA hybrid sites. *Nature* 468:713–16
147. Fischer N, Konevega AL, Wintermeyer W, Rodnina MV, Stark H. 2010. Ribosome dynamics and tRNA movement by time-resolved electron cryomicroscopy. *Nature* 466:329–33
148. Valle M, Zavialov A, Sengupta J, Rawat U, Ehrenberg M, Frank J. 2003. Locking and unlocking of ribosomal motions. *Cell* 114:123–34
149. Zhang W, Dunkle JA, Cate JH. 2009. Structures of the ribosome in intermediate states of ratcheting. *Science* 325:1014–17
150. Dunkle JA, Wang L, Feldman MB, Pulk A, Chen VB, et al. 2011. Structures of the bacterial ribosome in classical and hybrid states of tRNA binding. *Science* 332:981–84
151. Tama F, Valle M, Frank J, Brooks CL III. 2003. Dynamic reorganization of the functionally active ribosome explored by normal mode analysis and cryo-electron microscopy. *Proc. Natl. Acad. Sci. USA* 100:9319–23
152. Fei J, Kosuri P, MacDougall DD, Gonzalez RL Jr. 2008. Coupling of ribosomal L1 stalk and tRNA dynamics during translation elongation. *Mol. Cell* 30:348–59
153. Fei J, Bronson JE, Hofman JM, Srinivas RL, Wiggins CH, Gonzalez RL Jr. 2009. Allosteric collaboration between elongation factor G and the ribosomal L1 stalk directs tRNA movements during translation. *Proc. Natl. Acad. Sci. USA* 106:15702–7
154. Cornish PV, Ermolenko DN, Staple DW, Hoang L, Hickerson RP, et al. 2009. Following movement of the L1 stalk between three functional states in single ribosomes. *Proc. Natl. Acad. Sci. USA* 106:2571–76
155. Tsai A, Uemura S, Johansson M, Puglisi EV, Marshall RA, et al. 2013. The impact of aminoglycosides on the dynamics of translation elongation. *Cell Rep.* 3:497–508
156. Wang L, Pulk A, Wasserman MR, Feldman MB, Altman RB, et al. 2012. Allosteric control of the ribosome by small-molecule antibiotics. *Nat. Struct. Mol. Biol.* 19:957–63
157. Ermolenko DN, Spiegel PC, Majumdar ZK, Hickerson RP, Clegg RM, Noller HF. 2007. The antibiotic viomycin traps the ribosome in an intermediate state of translocation. *Nat. Struct. Mol. Biol.* 14:493–97
158. Menger M, Eckstein F, Porschke D. 2000. Dynamics of the RNA hairpin GNRA tetraloop. *Biochemistry* 39:4500–7
159. Johnson JE Jr, Hoogstraten CG. 2008. Extensive backbone dynamics in the GCAA RNA tetraloop analyzed using ^{13}C NMR spin relaxation and specific isotope labeling. *J. Am. Chem. Soc.* 130:16757–69
160. Zhao L, Xia T. 2007. Direct revelation of multiple conformations in RNA by femtosecond dynamics. *J. Am. Chem. Soc.* 129:4118–19
161. DePaul AJ, Thompson EJ, Patel SS, Haldeman K, Sorin EJ. 2010. Equilibrium conformational dynamics in an RNA tetraloop from massively parallel molecular dynamics. *Nucleic Acids Res.* 38:4856–67

162. Jucker FM, Heus HA, Yip PF, Moors EH, Pardi A. 1996. A network of heterogeneous hydrogen bonds in GNRA tetraloops. *J. Mol. Biol.* 264:968–80
163. Zhang YF, Zhao X, Mu YG. 2009. Conformational transition map of an RNA GCAA tetraloop explored by replica-exchange molecular dynamics simulation. *J. Chem. Theory Comput.* 5:1146–54
164. Goh GB, Knight JL, Brooks CL III. 2013. pH-dependent dynamics of complex RNA macromolecules. *J. Chem. Theory Comput.* 9:935–43
165. Leulliot N, Varani G. 2001. Current topics in RNA–protein recognition: control of specificity and biological function through induced fit and conformational capture. *Biochemistry* 40:7947–56
166. Xia T. 2008. Taking femtosecond snapshots of RNA conformational dynamics and complexity. *Curr. Opin. Chem. Biol.* 12:604–11
167. Hermann T, Patel DJ. 2000. Adaptive recognition by nucleic acid aptamers. *Science* 287:820–25
168. Tan D, Marzluff WF, Dominski Z, Tong L. 2013. Structure of histone mRNA stem-loop, human stem-loop binding protein, and 3′hExo ternary complex. *Science* 339:318–21
169. Stelzer AC, Frank AT, Kratz JD, Swanson MD, Gonzalez-Hernandez MJ, et al. 2011. Discovery of selective bioactive small molecules by targeting an RNA dynamic ensemble. *Nat. Chem. Biol.* 7:553–59
170. Woodson SA. 2010. Compact intermediates in RNA folding. *Annu. Rev. Biophys.* 39:61–77
171. Frieda KL, Block SM. 2012. Direct observation of cotranscriptional folding in an adenine riboswitch. *Science* 338:397–400
172. Duncan CD, Weeks KM. 2010. Nonhierarchical ribonucleoprotein assembly suggests a strain-propagation model for protein-facilitated RNA folding. *Biochemistry* 49:5418–25
173. Stern S, Changchien LM, Craven GR, Noller HF. 1988. Interaction of proteins S16, S17 and S20 with 16S ribosomal RNA. *J. Mol. Biol.* 200:291–99
174. Ramaswamy P, Woodson SA. 2009. S16 throws a conformational switch during assembly of 30S 5′ domain. *Nat. Struct. Mol. Biol.* 16:438–45
175. Whitford PC, Geggier P, Altman RB, Blanchard SC, Onuchic JN, Sanbonmatsu KY. 2010. Accommodation of aminoacyl-tRNA into the ribosome involves reversible excursions along multiple pathways. *RNA* 16:1196–204
176. Eichhorn CD, Feng J, Suddala KC, Walter NG, Brooks CL III, Al-Hashimi HM. 2012. Unraveling the structural complexity in a single-stranded RNA tail: implications for efficient ligand binding in the prequeuosine riboswitch. *Nucleic Acids Res.* 40:1345–55
177. Suddala KC, Rinaldi AJ, Feng J, Mustoe AM, Eichhorn CD, et al. 2013. Single transcriptional and translational $preQ_1$ riboswitches adopt similar pre-folded ensembles that follow distinct folding pathways into the same ligand-bound structure. *Nucleic Acids Res.* 41:10462–75
178. Sim AY, Levitt M. 2011. Clustering to identify RNA conformations constrained by secondary structure. *Proc. Natl. Acad. Sci. USA* 108:3590–95
179. Nissen P, Ippolito JA, Ban N, Moore PB, Steitz TA. 2001. RNA tertiary interactions in the large ribosomal subunit: the A-minor motif. *Proc. Natl. Acad. Sci. USA* 98:4899–903
180. Doherty EA, Batey RT, Masquida B, Doudna JA. 2001. A universal mode of helix packing in RNA. *Nat. Struct. Biol.* 8:339–43
181. Sattin BD, Zhao W, Travers K, Chu S, Herschlag D. 2008. Direct measurement of tertiary contact cooperativity in RNA folding. *J. Am. Chem. Soc.* 130:6085–87
182. Behrouzi R, Roh JH, Kilburn D, Briber RM, Woodson SA. 2012. Cooperative tertiary interaction network guides RNA folding. *Cell* 149:348–57
183. Das R, Travers KJ, Bai Y, Herschlag D. 2005. Determining the Mg^{2+} stoichiometry for folding an RNA metal ion core. *J. Am. Chem. Soc.* 127:8272–73
184. Mustoe AM, Al-Hashimi HM, Brooks CL III. 2014. Coarse grained models reveal essential contributions of topological constraints to the conformational free energy of RNA bulges. *J. Phys. Chem. B.* In press

Annual Review of Biochemistry
Volume 83, 2014

Contents

Journeys in Science: Glycobiology and Other Paths
Raymond A. Dwek 1

Lipids and Extracellular Materials
William Dowhan 45

Topological Regulation of Lipid Balance in Cells
Guillaume Drin 51

Lipidomics: Analysis of the Lipid Composition of Cells and Subcellular Organelles by Electrospray Ionization Mass Spectrometry
Britta Brügger 79

Biosynthesis and Export of Bacterial Lipopolysaccharides
Chris Whitfield and M. Stephen Trent 99

Demystifying Heparan Sulfate–Protein Interactions
Ding Xu and Jeffrey D. Esko 129

Dynamics and Timekeeping in Biological Systems
Christopher M. Dobson 159

Metabolic and Nontranscriptional Circadian Clocks: Eukaryotes
Akhilesh B. Reddy and Guillaume Rey 165

Interactive Features of Proteins Composing Eukaryotic Circadian Clocks
Brian R. Crane and Michael W. Young 191

Metabolic Compensation and Circadian Resilience in Prokaryotic Cyanobacteria
Carl Hirschie Johnson and Martin Egli 221

Activity-Based Profiling of Proteases
Laura E. Sanman and Matthew Bogyo 249

Asymmetry of Single Cells and Where That Leads
Mark S. Bretscher 275

Bringing Dynamic Molecular Machines into Focus by Methyl-TROSY NMR
Rina Rosenzweig and Lewis E. Kay 291

Chlorophyll Modifications and Their Spectral Extension in Oxygenic Photosynthesis
Min Chen 317

Enzyme Inhibitor Discovery by Activity-Based Protein Profiling
Micah J. Niphakis and Benjamin F. Cravatt 341

Expanding and Reprogramming the Genetic Code of Cells and Animals
Jason W. Chin 379

Genome Engineering with Targetable Nucleases
Dana Carroll 409

Hierarchy of RNA Functional Dynamics
Anthony M. Mustoe, Charles L. Brooks, and Hashim M. Al-Hashimi 441

High-Resolution Structure of the Eukaryotic 80S Ribosome
Gulnara Yusupova and Marat Yusupov 467

Histone Chaperones: Assisting Histone Traffic and Nucleosome Dynamics
Zachary A. Gurard-Levin, Jean-Pierre Quivy, and Geneviève Almouzni 487

Human RecQ Helicases in DNA Repair, Recombination, and Replication
Deborah L. Croteau, Venkateswarlu Popuri, Patricia L. Opresko, and Vilhelm A. Bohr 519

Intrinsically Disordered Proteins and Intrinsically Disordered Protein Regions
Christopher J. Oldfield and A. Keith Dunker 553

Mechanism and Function of Oxidative Reversal of DNA and RNA Methylation
Li Shen, Chun-Xiao Song, Chuan He, and Yi Zhang 585

Progress Toward Synthetic Cells
J. Craig Blain and Jack W. Szostak 615

PTEN
Carolyn A. Worby and Jack E. Dixon 641

Regulating the Chromatin Landscape: Structural and Mechanistic Perspectives
Blaine Bartholomew 671

RNA Helicase Proteins as Chaperones and Remodelers
Inga Jarmoskaite and Rick Russell 697

Selection-Based Discovery of Druglike Macrocyclic Peptides
Toby Passioura, Takayuki Katoh, Yuki Goto, and Hiroaki Suga 727

Small Proteins Can No Longer Be Ignored
Gisela Storz, Yuri I. Wolf, and Kumaran S. Ramamurthi 753

The Scanning Mechanism of Eukaryotic Translation Initiation
Alan G. Hinnebusch 779

Understanding Nucleic Acid–Ion Interactions
Jan Lipfert, Sebastian Doniach, Rhiju Das, and Daniel Herschlag 813

Indexes

Cumulative Index of Contributing Authors, Volumes 79–83 843

Cumulative Index of Article Titles, Volumes 79–83 847

Errata

An online log of corrections to *Annual Review of Biochemistry* articles may be found at http://www.annualreviews.org/errata/biochem